FORMATION AND COMBUSTION CHARACTERISTICS OF ELEPHANTGRASS AND ENERGYCANE WAFERS

By

MOHAMAD I. MOFLEH

A DISSERTATION PRESENTED TO THE GRADUATE SCHOOL
OF THE UNIVERSITY OF FLORIDA IN PARTIAL FULFILLMENT
OF THE REQUIREMENTS FOR THE DEGREE OF
DOCTOR OF PHILOSOPHY

UNIVERSITY OF FLORIDA

1997

ACKNOWLEDGMENTS

I would like first to express my deep gratitude to my supervisor, Dr. Larry O. Bagnall, from whom I learned a lot. He guided me in a professional and dedicated manner throughout my work. I also would like to express my appreciation to my committee members Drs. Shaw, Fluck, Kiker and Green, who were always there to answer my questions and contribute with their expertise to this research. Thanks are extended to the technicians in the shop of the ABE for a well-done job.

I am thankful to Drs. H. El-Shal, F. Ebrahimi, A. Wilkie and their graduate students for the help they provided. Thanks also go to the Department of Soil and Water Sciences who provided part of the chemical analyses of the material samples.

The endless love, encouragement and support of my parents and family pushed me foreword throughout my academic progress. They cannot be adequately acknowledged with words. The encouragement of my friends is also sincerely acknowledged.

I am indebted to the Jordan University of Science and Technology, Irbid, Jordan, for their financial support during my graduate studies. Finally, the pleasant spirit and open-mindedness of Dr. G.H. Smerage made working with him a useful as well as joyful experience. The financial assistance he provided is highly appreciated.

TABLE OF CONTENTS

LIST OF TABLES

LIST OF FIGURES

KEY TO SYMBOLS AND ABBREVIATIONS

σ, P:	stress, pressure
ρ:	material density
ρ_{max}:	maximum density
ρ_i:	instantaneous density
ρ_0:	initial density
ρ_f:	final (relaxed) density
ρ_m:	immediate density
u:	non-dimensional density
a, b, C, c:	a constant or parameter
K, α, β:	a constant or parameter
MC:	moisture content
P_{max}:	maximum stress (pressure)
W:	wafer weight (charge)
A:	cross-sectional area
D_c:	die diameter
y:	deformation
H:	wafer height

t_h:	hold (dwell) time
F:	force
E:	energy
υ:	specific volume
X_{max}:	maximum relative expansion
π_i:	a non-dimensional variable group (pi term)
R_c^2:	correlation coefficient
R_d^2:	coefficient of determination
V:	velocity
g:	acceleration due to gravity
K.E.:	kinetic energy
τ:	shear stress
A_s:	surface area
F_s:	shearing force
HV:	heating value
T_s:	stack temperature
T_f:	flue gases temperature
T_i:	insulation temperature
T_a:	ambient temperature
P_a:	ambient pressure
η_h:	stove efficiency
m:	mass

c_p: specific heat

ΔT: temperature difference

DM: dry matter

Abstract of Dissertation Presented to the Graduate School
of the University of Florida in Partial Fulfillment of the
Requirements for the Degree of Doctor of Philosophy

FORMATION AND COMBUSTION CHARACTERISTICS OF ELEPHANTGRASS AND ENERGYCANE WAFERS

By

Mohamad I. Mofleh

August 1997

Chairperson: Larry O. Bagnall
Major Department: Agricultural and Biological Engineering

Elephantgrass (*Pennisetum purpureum* Schum.) and energycane (*Saccharum* Spp.) are two cane type grasses. These are tall-growing perennial bunchgrasses that produce long hardened stems and grow in the tropics and subtropics. Traditionally, they have been used for forage and, in some regions, have been randomly burned on fields or disposed of uselessly. However, these plants have high dry matter yield and, thus, are excellent candidates as energy crops.

Elephantgrass and energycane have been used for direct combustion in their loose form in large-scale applications. Several problems, many of which were attributed to their low bulk density, were encountered with using the materials.

Consequently, this project was initiated to investigate the formation and combustion characteristics of the two materials in the form of small compact units called wafers.

A hydraulic press that applied axial stresses on the material in four different dies was used. A load cell and a displacement transducer were utilized to measure the stresses and material deflection. Wafer quality was evaluated using a tumbler built according to the American Society of Agricultural Engineers standards. In addition, a small stove was built to test wafer combustion. Thermocouples were used to measure temperatures during combustion. All the data gathered was transferred to a computer using a data acquisition system.

It was found that the stress-deformation and stress-density relationships of elephantgrass and energycane were of exponential nature. Compaction energy required, which was calculated from the area under the force-deformation curves, ranged from 0.1 to 0.3% of their energy content. It was also found that wafer quality (durability) was mainly a function of wafer size and its final (relaxed) density in addition to material stem-to-leaf ratio and its crude protein content.

Wafers possessed poor ignition quality but once ignited, they burned satisfactorily. The results indicated that sufficient and uniform combustion air distribution and a stove lining were critical factors in burning these materials. Further, the findings revealed that it may not be recommended to use elephantgrass or energycane in large-scale applications due to their high slagging index. Nonetheless, using them in small-scale applications may be possible. Elephantgrass was generally a better candidate for such an application.

CHAPTER 1
INTRODUCTION

Estimates that fossil fuel resources, natural gas and oil in particular, will be used up in the near future along with serious pollution problems associated with their use (Balatinecz, 1983) have triggered intensive research efforts to look for new alternative energy sources. Biomass energy sources are among the most promising. They are renewable, safer to store and handle, environment friendly, available and distributed in almost all regions of the world, and in some cases are cheaper than others (Salter, 1982; White and Plaskett, 1981; Reed et al., 1980).

A wide range of biomass-based sources has been investigated. The literature covers such areas as municipal and agricultural wastes, plant oils, forest and agricultural residues, and wood materials, to mention a few. Still, biomass sources have been a minor contributor. In the U.S., only 3 exajoules (EJ) are produced from biomass compared to a potential of 10 to 15 EJ or about 15% of the total 84 EJ of energy consumed (Green et al., 1991).

Based on an extensive literature search, cane type grass species such as elephantgrass or napiergrass (*Pennisetum purpureum* Schum.) and energycane (*Saccharum* spp.) in densified form have not been investigated as to their potential as a

feasible energy source. Yet, they have been studied for methane production and direct combustion in loose form (Woodard and Prine, 1992; Tuhoy and Jihasz, 1994). Traditional uses of these grass species have been either as ingredients in livestock's rations (Woodard et al., 1985), or, in some areas, random on-field burning (O'Dougherty and Wheeler, 1984). Clearly, some benefits (as well as problems) are associated with these uses but it is realized that there is room for potentially more useful and efficient ways to use these species. Therefore, it is felt that an attempt to systematically study processing the grass in such a form that makes it possible for controlled burning is worthwhile.

A major problem of forage materials handling and utilization, including grass, is the high cost. This is primarily due to the large volume required for their transportation and storage, which in turn is attributed to the inherent low bulk density of such materials (Salter, 1982; Smith, 1987). Another major problem is the high cost of processing these materials, particularly if the end-use of the material is not rewarding (Reed et al., 1980). In fact, bales, the traditional form of hay, exemplify these arguments.

In an attempt to minimize these problems, this research project involved compressing and densifying the chopped material under relatively high axial pressures. The principal goal of material densification was to transform its loose structure into a dense self-contained package called a "cube" or "wafer." This technology is well established and has been used in related or similar applications such as the feed industry (Bhattacharya et al., 1989). The densified form offers the advantages of higher bulk

density and thus lower costs of transportation and storage; reduces losses and increases the volumetric energy content, also known as energy density, of the material (Bhattacharya et al., 1989; O'Grady et al., 1980). Densification also converts the material into a product of uniform size and quality, which lends itself readily to mechanical handling and results in less labor costs. Further, by wafering rather than pelleting, the costly grinding process required for pelleting was avoided (Dobie, 1960).

Energy or power requirement is an important factor in determining the total cost of the process. The energy efficiency of densification processes is fairly high. Balatinecz (1983) estimated the energy efficiency of biomass densification between 82 to 93%. Beck and Halligan (1980) looked at this aspect from a different perspective and indicated that only 5 to 10% of the material energy content was required for compaction. The method of compression utilized in this work took this factor into account. Extrusion and compression in a closed-end die are the two main types of machines used for compaction. Both configurations are shown in Fig. (1-1).

Extrusion, which is dominant in commercial plants, is such an energy-wasteful process because of the high friction involved in the ejection process (Reece, 1965). In contrast, closed-end die compression is much less energy demanding and, therefore, was used in this study. It requires as little as 25% to 33% of the energy required for extrusion machines (Bellinger et al., 1961; Pickard et al., 1961). In addition, the load was applied steadily because it was proven to be more efficient than impact loads (Chancellor, 1961).

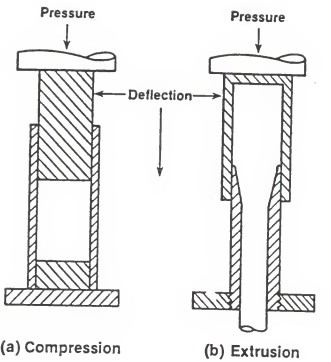

Fig. 1-1. Schematic representation of densification configurations (Source: Miles et al., 1980).

Because no data was found on compressing the grass species considered here or burning them in the compressed form, this research effort included an attempt to experimentally (empirically) determine the optimum conditions for compressing elephantgrass and energycane and relate that to the manner in which they burn. Moreover, the compact form of the material facilitated feeding the material into the combustion apparatus. Feeding densified material was easier and more efficient than feeding the same amount of loose biomass material. Previous studies with biomass fuels

in large-scale applications reported such problems as bridging of material in the feeding system, the need for large feeding hoppers, and the need for frequent feeding (Green et al., 1991; Tuhoy and Jihasz, 1994). Some of these drawbacks may be encountered in small-scale applications as well.

The importance of this work stems mainly from the fact that no previous work has been found that addresses this problem in a systematic way. Moreover, the current low price of oil is not a solution to the energy problem. This work offered a chance to address a whole new category of species of biomass materials as a potential source of energy particularly in small-scale applications such as residential heating. Put another way, the work was based on the underlying assumptions that raw material biomass such as the species considered here is available on farms in sufficient quantities and that other possible energy sources are either too expensive or hard to obtain.

This may best fit developing countries because the above circumstances may well exist. Additionally, these species are not basic food items, and the level of technological sophistication of the process is not high, especially for small-scale applications. Moreover, establishing these crops as fuel provides a substitute for fuel wood. Wood has been overused in many regions in the less developed world, which has caused serious problems of deforestation and desertification (Bhattacharya, 1989). In fact, the use of some biomass residues as an energy source has started to evolve in developing countries (Petrie and Baldwin, 1992).

The importance of this work may also be assessed based on the findings that will be realized by the end of this study. Knowledge of material compression

characteristics, compaction energy requirement and their suitability as fuel may help create more interest and motivate new serious research efforts that may realize better varieties of grass that fit this particular line of use. In addition, the current compression technology may be improved and new techniques for their processing and utilization may be devised. This includes less energy-consuming compression methods, thus making these grass species more attractive as an energy source by lowering the costs associated with their handling and processing. Parallel studies may be initiated to increase the yield and optimize the production of these grasses.

Possible benefits of this research include new uses of these species and an attempt to utilize them to their full potential as it is believed that traditional uses do not meet this condition. This argument applies in particular where these grasses are disposed of uselessly or the material is randomly burned in the field. Further, the knowledge projected to be acquired by the end of this work may be applied in other possible application areas such as the feed industry. Moreover, once it is proved that these species are a promising source of energy, economic benefits must be realized by the agricultural community by creating new markets and increasing the demand for these materials. Idle acreage or portions of farms may be used to cover the energy needs of farmers. In other words, as a renewable source that can be made available on farms, these grasses can be utilized, for instance, as an emergency fuel for residential uses such as on-farm heating and in some regions and under simple settings for home cooking.

Objectives

The overall objective of this dissertation was to study the characteristics of formation of elephantgrass and energycane wafers and investigate their potential as a fuel source in their compact form by examining the manner in which they burn. The specific objectives of this research can be summarized as follows:

1. To study the formation characteristics of grass wafers in regard to their pressure-density behavior under axial pressure (stress) on a laboratory scale. A comparison of these experimental results with existing models and results with other materials will be made.

2. To evaluate product quality in terms of its durability (its ability to withstand handling) and stability (the wafer post-compression expansion with time).

3. To investigate the combustion characteristics of the species considered as a step in determining their feasibility as a possible source of energy. The main criteria will be stove temperature and performance, slagging potential, the sustainability of the burning process.

4. To attempt to correlate the formation parameters and combustion characteristics and explore the areas of possible improvements in the process.

5. To compare the two materials in terms of their potential as a source of energy to determine the most feasible one(s).

It is to be emphasized, though, that the species considered in this research may generally be a different category of grass compared to those investigated in the past. These species are larger and can be classified as "woody" grasses and may deviate from the behavior of other species presented in the literature.

The main body of this dissertation was organized in such a way to cover these objectives in a manner that was compatible with the sequence of material compaction. Chapter 2 presents a survey of relevant aspects reported in the literature on similar or related applications. Chapter 3 includes a description of the materials and methods and experimental procedures utilized in this work, which included experimental setup, equipment, and methods of parameter measurement. The wafer formation characteristics and its quality were presented in chapters 4 and 5. An assessment of the combustion characteristics of the material in its consolidated form is presented in chapter 6. Finally, a brief summary of the major findings of this study is found in chapter 7.

CHAPTER 2
LITERATURE REVIEW

Introduction

No study has been found that approaches these grasses in consolidated form from the viewpoint of combustion or as a source of energy. However, there is a fair amount of work done on forage materials, alfalfa in particular, to evaluate their potential as livestock feed in pelleted or wafered form especially in the 1950s and 1960s. These efforts were aimed primarily at realizing the benefits of reducing the costs of handling of these materials (Willits et al., 1969).

In many cases the terms "pellets" and "wafers" or "cubes" are used interchangeably and no consistent standard is followed in differentiating the two (Shepperson and Grundey, 1962). However, it is generally accepted that pellets refer to the cylindrical dense packages made from finely ground materials while wafers or cubes refer to the disk-shaped packages made from chopped or long forage material and are, in general, less dense than pellets (Molitorisz et al., 1968; Shepperson and Grundey, 1962; Butler et al., 1961). Yet, the American Society of Agricultural Engineers (ASAE) has presented the following definition for pellets:

"An agglomeration of individual ground ingredients, or mixture of such ingredients, commonly used for animal feeds." (ASAE S269.4, 1996). In this text, the term wafer(s) will be used throughout. It is intended to refer to the consolidated grass packages made from applying an axial force in a closed-end die compression system onto the loose grass material that may be long or chopped. The resulting product is to be used as a source of energy by burning it in a small stove typical of those used in residential heating.

Elephantgrass or napiergrass (*Pennisetum purpureum* Schum.) and energycane (*Saccharum* spp.) are two good representatives of the so-called tall or cane type grasses. These are tall-growing perennial bunch grasses and utilize the C4 pathway of carbon fixation and produce long hardened stems (Woodard et al., 1993). They grow in subtropical and tropical regions and were recognized as having an excellent potential for energy production by direct combustion. They were also considered among the most energy-efficient herbaceous plants grown in the tropics (Smith, 1987). In fact, they both fall under the category of energy crops in the so-called energy farming due to the fact that their dry matter (DM) yields, which exceeds 40 Mg per hectare per year, are considered high compared to most other plants (Woodard and Prine, 1993). In energy terms, and based on an average heating value of 17200 kJ/kg, this is approximately equivalent to 700,000 MJ per hectare per year.

Mechanics and Characteristics of Forage Deformation

Introduction

Mechanical properties of materials are those that define their behavior under applied loads (forces). For most materials, the nature of the applied load is the primary factor in defining the material's response. However, for most biological materials, such as forages, the deformation and flow (creep) in the material depends on time, in addition to load (Sitkei, 1986). Such materials are classified as rheological. The term rheology has been defined as the study of deformation and flow of materials under the action of forces taking time effects into consideration (Henderson and Perry, 1976). Ideally, a material under load may respond in one of three ways: elastic, plastic, or viscous. Thus, the basic properties that define the rheological behavior of materials are their elasticity, plasticity, and viscosity (Heldman, 1975).

In reality, however, materials deviate from these idealizations. This is particularly true for agricultural materials, which exhibit a stress-deformation relationship that depends on strain rate as well as strain. This introduces a time dependency and such materials are termed viscoelastic. These materials exhibit solid-like and liquid-like characteristics simultaneously (Graham and Bilanski, 1984). This agrees with the fact that the basic structural element of biological materials is the cell which consists of an external solid wall and an internal fluid (Moustafa et al., 1966).

For a material, the stress-strain ratio may depend on time alone or on time as well as the magnitude of stress. In the former case, the material is classified as linearly viscoelastic and in the latter the material is said to be non-linear viscoelastic. Most biological materials fall in the category of non-linear viscoelastic materials (Graham and Bilanski, 1984; Hundtoft and Buelow, 1971) and modeling of biological materials as linear viscoelastic serves only as a quantitative approximation of their actual behavior (Faborode and O'Callaghan, 1989).

One of the most important aspects of the mechanics of forage deformation in relation to wafering, in addition to stress-strain-time relationships, is the possibility of translating a stress-deformation relationship into a pressure (stress)-density relationship. Such a relationship, under a given set of process parameters and material properties, is fundamental to optimizing the wafering process in regard to machine design and energy requirement (Faborode and O'Callaghan, 1986). Moreover, pressure, σ, is a significant process variable in the wafering process while wafer density, ρ, is of prime importance in determining the quality of wafers in terms of their stability and durability (Hill and Pullkinen, 1988). This will be shown to be the case in subsequent chapters when formation characteristics and wafer quality are discussed.

Stress-Density Relationship

The applied axial pressure, σ, has pronounced influence on the wafer density. Butler et al. (1959) came up with the following relationship:

$$\rho = K_1 \ln\left(\frac{\sigma}{K_2}\right) \tag{2-1}$$

where K_1 and K_2 are material parameters.

Reece (1965) found a linear stress-density relationship ($\rho = k\sigma$) when worked with chopped alfalfa up to 13 MPa (2000 psi). Bilanski et al. (1985) cited Neuman (1975) who reported based on a study by Skalweit (1938) that

$$\sigma = C(\rho)^m \tag{2-2}$$

where C and m are parameters.

Bilanski et al. (1985) criticized both Eqns. (1) and (2) as purely empirical, limited in range and restricted in application. Based on analytical analysis, they ended up with the following general relationship

$$u = \frac{\rho_{max} - \rho}{\rho_{max} - \rho_0} = \exp\left(-\frac{\sigma}{K}\right) \tag{2-3}$$

where K is a parameter

u is the dimensionless wafer density

ρ_{max} is the ultimate density under a given σ

ρ_0 is the material initial density

O'Dougherty and Wheeler (1984) indicated that the relationship between pressure, P, and density for wheat straw depended on density range. They presented the following two expressions. For $150 < \rho < 400$ kg/m^3

$$P=(C_1)(\rho)^2 \tag{2-4}$$

and for $\rho > 400$ kg/m3

$$lnP=C_2[\ln(\rho)]^4-C_3 \tag{2-5}$$

where C_1, C_2, and C_3 are empirical constants.

In a review of previous proposed models for the pressure-density relationship, Faborode and O'Callaghan (1986) presented the results of several workers. The authors cited the work of Osobov (1967) who obtained the following formula

$$P=\frac{C}{a}[\exp(a(\rho-\rho_0))-1] \tag{2-6}$$

where C and a are empirical constants. Faborode and O'Callaghan (1986) also cited the work of Mewes (1958) who modified an expression first proposed by Skalweit (1938) and obtained the following expression:

$$P=C(\rho-\rho_0)^m \tag{2-7}$$

where C and m are empirical constants.

However, these expressions were criticized by Faborode and O'Callaghan (1986) as relying on empirical constants and not including material characteristics or

process properties. Therefore, based on analytical analysis, they proposed the so-called compression-ratio model to overcome the shortcomings of previous models. The model equation was

$$P=\frac{K_0}{b}[(\exp(b(r-1))-1] \tag{2-8}$$

where K_0 is the bulk modulus

b is the material porosity or percent of voids

r is the compression ratio

In Eqn. (2-8), K_0 is a measure of the material volumetric incompressibility, b measures the degree of packing and r was defined as the ratio of density at any instant during compression to the initial density.

Many researchers studied the creep and stress relaxation properties of biological materials under axial stress. They employed rheological models to investigate the behavior of these materials as linear (Rehkugler and Buchele, 1967; Kjelgaard et al., 1976) or nonlinear viscoelastic (Faborode and O'Callaghan, 1989 ; Bilanski and Graham, 1984). All these models consisted of a combination of mechanical elements, mainly springs and dashpots. The most common of these models are the Kelvin model, the Maxwell model, and the Burges model.

Creep curves, which portray material strain with time, were developed and consisted of two phases. The first was the creep deformation which was due to holding the material under a given maximum pressure (constant stress) for a given period of

time, known as hold or dwell time. The second phase was the creep recovery which was closely tied to the material stress relaxation. Creep recovery describes material expansion with time, which occurs upon unloading (constant strain) (Kjelgaard et al., 1976) and stress relaxation refers to dissipation of stress from the material during loading and after the load has been removed. The creep curve is an important tool in optimizing the hold time for densification of materials (Mohsenin and Zaske, 1976).

Factors Affecting the Wafering Process

The parameters and variables involved in the wafering process have been extensively investigated. There is a general trend to divide these variables into two categories (Reece, 1965; Balk, 1965; Rundell et al., 1962; Witte et al., 1961):

1. Those associated with the machine such as maximum pressure or stress (P), dwell (hold) time (t_h), loading or compression rate, and die geometry.

2. Those associated with the material to be wafered such as moisture content (MC), charge (W) and particle size.

The most important factors among these are moisture content, maximum pressure, die diameter and hold time, in that order. In fact, the parameters mentioned above are those that will be considered in this project at one or more levels. There are a few more variables not included in this work such as the influence of the temperature of material and/or die and the use of binding materials. In the wafering process, all the variables mentioned above are interrelated in light of the fact that the ultimate goal of the

material compaction is a dense, stable, and durable product (Reece, 1965; Rundell and Fairbanks, 1967).

Maximum pressures, P_{max}, used in previous investigations with forage materials ranged from about 14 to 70 MPa (2,000 to 10,000 psi). The P_{max} is closely tied to wafer density. The general trend was that higher maximum pressure resulted in denser wafers. Bruhn (1959) and Bruhn et al. (1959) working with alfalfa reported this trend. Similar results were reported by several other researchers (Reece, 1969). Rundell and Fairbanks (1967) arrived at the same result and concluded that the maximum pressure is determined by the desired density. Smith et al. (1977) working with wheat straw reported higher densities with higher pressures and added that higher pressures resulted in more expansion. It is noteworthy that higher maximum pressure requires more energy (Bellinger and McColly, 1961). Therefore, several researchers attempted to establish optimum maximum pressure ranges for different materials (Shepperson and Grundey, 1962).

Hold time, t_h, also known as dwell or retention time, is the time the material is held under maximum pressure, P_{max}. It had similar effect as that of P_{max}, namely, increasing the hold time increased the wafer density and stability (Bruhn, 1959). Butler (1959) indicated a linear relationship between wafer density and the logarithm of t_h. Hold times used in previous studies ranged between 0.05 seconds (impact) up to twenty five seconds.

Exceeding the optimum t_h of a material led to higher rates of wafer expansion and, like P_{max}, meant a waste of energy (Bruhn et al., 1959). Several workers

established optimum hold times for different materials, most of which fell in the range of 5 to 25 seconds (Faborode and O'Callaghan, 1987; Reece, 1965; Dobie, 1960; Butler and McColly, 1959). The time-dependent response of alfalfa and grass was studied by Graham et al., (1984). They suggested that the hold time be limited to a maximum of 5 seconds as most of the increase in density with time was achieved within this time duration, that is, within the transient response of these materials.

Loading rate or compression speed, which is essentially the speed of the ram while approaching and pressing the material, is closely tied to the dwell time. Chancellor (1962) studied and compared both impact and quasi-static loading and concluded that impact was less efficient than static (quasi-static) loading. Faborode and O'Callaghan (1987) suggested that high ram speeds required more energy and were not efficient in the material compaction because there was not enough time for a permanent deformation to occur in the material.

The term charge is used to refer to the amount (weight or volume) of the material filled in the die to make a single wafer. Butler and McColly (1959) indicated that increasing the volume of material "to a degree" increased density and attributed that to the increase in number of interlocking fibers. However, increasing the charge beyond acceptable limits had unfavorable consequences. Dramatic increases in the required maximum pressure with increasing charge were reported (Gustafson and Kjelgaard, 1962). This conclusion was confirmed by Faborode and O'Callaghan (1987) who indicated that increasing the charge resulted in more friction and less pressure transmissibility through the material. This resulted, they explained, in poor binding

and, thus, less cohesive product. Dobie (1960) claimed that the optimum wafer shape in terms of flow characteristics had a length to diameter ratio of unity which in most cases dictates an increase in charge. A compromise between wafer quality and flow characteristics should be sought.

Die geometry describes the shape and dimensions of the compression die. The vast majority of dies used in the pelleting and wafering industry and investigations are cylindrical. In a study in which they compared several wafer (die) shapes, Gustafson and Kjelgaard (1962) concluded that cylindrical wafers had better characteristics than spherical in terms of stability and energy consumption. For a compaction machine with a given load capacity, the dimensions of the die determine its cross sectional area. For a cylindrical die, the diameter is the dimension of interest. This reflects on the maximum attainable pressure on the material which influences the wafer quality in the manner discussed earlier. Generally speaking, smaller dies produced a better product (Hill and Pullkinen, 1988; Butler and McColly, 1959). Thus, in most previous studies, the die diameter did not exceed 76 mm (3 inches).

Moisture content (MC) of the material was singled out as the most important factor in the wafering process (Rehkugler et al., 1969; Balk, 1964; Smith et al., 1971). Optimum moisture contents for wafering (pelleting) forage materials were reported and fell in the range 10% to 25%, wet basis (Bilanski et al., 1984; Reece, 1965; Balk, 1965; Dobie, 1960 and 1959). MC had great influence on the energy requirement and stability of wafers. Most researchers showed an increase in maximum pressure and energy consumption with an increase in MC beyond the optimum range with a

considerable post-compression expansion (Bruhn, 1955; Bruhn et al., 1959; Bellinger and McColly, 1961; Witte et al., 1961; Mohsenin et al., 1976).

Several workers theorized that high moisture was trapped within the forage material and, being incompressible, prevented the breakdown of the material structure. This resulted in high elasticity, hence lower permanent strains and less stable pellets (Huang and Yoerger, 1961). Faborode and O'Callaghan (1987) added that excess moisture raised the pore pressure and reduced the net pressure on the material.

Faborode and O'Callaghan (1987) indicated that mechanical properties of biological materials were strong functions of MC. Further, the axial stress, σ, was directly related to moisture content, MC, in modeling the compaction of forage materials. A simple quadratic equation was obtained for the σ-MC by Hall and Hall (1967). Based on a statistical analysis of experimental data, Hundtoft and Buelow (1971) proposed the following model for alfalfa:

$$\sigma=(\frac{b_1}{MC^2})(MC-\frac{b_2 W}{A})(\epsilon+b_3 MC)^{b_4+b_5 MC} \qquad (2\text{-}9)$$

where b_i are material parameters, i = 1, 2, ..., 5

W/A is material weight per unit cross-sectional area of compression chamber

ϵ is the axial strain.

While low moisture adversely affects the waferability of a material (Bruhn, 1959), increasing moisture within the optimum range had favorable effects in terms of the required energy and maximum pressure by making the material more pliable and easier

to deform (Gustafson and Kjelgaard, 1962; Reece, 1965). Hill and Pullkinen (1988) explained the favorable effects of moisture by arguing that moisture added lubricity (less friction). Faborode and O'Callaghan (1987) claimed that some moisture was necessary to effect the material's natural binding.

Particle size, which is basically the length of cut of the material prior to wafering, is a pretreatment procedure that is normally brought about by mechanical degradation of the material. Many workers attached insignificant influence to particle size on wafering (Gustafson and Kjelgaard, 1962; Hall and Hall, 1967). Others reported positive effects of larger particle size on wafer quality (Hill and Pullkinen, 1988).

Thermal effects were reported as having a significant effect on wafer formation. Raising the material and/or die temperature by adding heat appreciably enhanced the wafering process as a whole. The higher temperature reduced pressure and energy required and still improved the wafer quality (Reece, 1965; Hall and Hall, 1967; Smith et al., 1976). Finally, using foreign binding materials did not, in general, influence the process (Hill and Pullkinen, 1988; Dobie, 1960; Headley, 1968) although in some cases, it was reported that it had favorable influence on wafer stability (Sah et al., 1980).

Although controversial, the self-bonding mechanism of the binderless densification process, as is the case in this research, most likely depends on both mechanical and natural bindings. Mechanical binding is represented by the interlocking and interlacing of the material fibers. Material natural binding comes from both the

pectin that is squeezed primarily under pressure and lignin and wax materials that soften and flow due to thermal effects represented by higher material temperature due to compression (Bhattacharya, 1989).

CHAPTER 3
MATERIALS AND METHODS AND EXPERIMENTAL PROCEDURES

This chapter covers the materials and methods that pertain to the material compaction. The information presented here is relevant to the discussions presented in chapter 4 and parts of chapter 5. The materials and methods and procedures regarding other aspects of this study are conveniently located where those aspects are discussed.

Material Collection and Pre-treatment

Late cut elephantgrass and energycane were harvested by hand between mid-December through February, 1995, from a plot in the Energy Park of the University of Florida. The material was harvested using a large knife, collected and transported by a truck to the shop. Both materials were mechanically chopped for size reduction, and then dried at an average temperature of about 60 C for 24 hours to bring its moisture content to approximately 10% wet basis (w.b.) to avoid spoilage and guarantee safe storage. The material was then filled in plastic bags and stored in open air for a period of 3 to 6 months. Both the chopping machine and forced-air batch drier used were

designed and fabricated in the Agricultural and Biological Engineering Department at the University of Florida (Dr. Larry O. Bagnall).

Prior to processing into wafers, the material was crushed and then chopped in a grinding machine (hammer mill) from W.W. Grinder Corp., using a 5-cm screen and again was stored in plastic bags under ambient conditions for an additional period of 1 to 4 weeks. Fig. (3-1) and Fig. (3-2) depict the crushing and grinding machines used in this work.

Fig. 3-1. The chopping machine used in this study to reduce material size.

Fig. 3-2. The grinder (hammer mill) used to cut material to a nominal size of 5 cm.

Material Compression

Experimental and Apparatus Setup

Pressing the loose material into compact cylindrical wafers was a major part of this work. An effort was made to come up with a simple but efficient system of compression. A 10-ton Enerpac hydraulic press equipped with a new ram with a 38-mm diameter piston was used to apply pressure. A schematic sketch of the

compression equipment is shown in Fig. (3-3). Four cylindrical dies (chambers) were fabricated with four different diameters, namely, 40, 50, 63, and 76 mm and a height of about 165 mm each. The dies had removable bases (lids) to allow for wafer ejection.

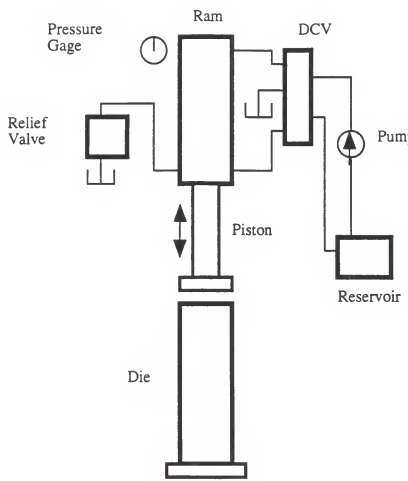

Fig. 3-3. A schematic sketch of the compression equipment (hydraulic ram and die).

To fit each die, four piston heads with different diameters of approximately 40, 50, 63 and 76 mm, were made. Each piston head was attached to the piston via a threaded joint. A 0.4 mm clearance was chosen between piston heads and die walls to allow air in the material void space to escape thus allowing more efficient compression.

Wafer ejection from the die was achieved by "ejection cups", which were in the form of supporting cylinders designed such that they would fit the lower end of the die in place of the replaceable base. The piston was used to push the wafer out of the die through the cup because, after compression, wafers would be stuck tightly in the die. The manner in which wafers were ejected is shown in Fig. (3-4).

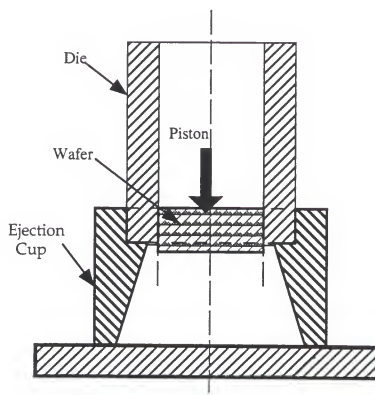

Fig. 3-4. A schematic sketch of wafer ejection.

During compression, two quantities were measured. The first was the piston displacement throughout the compression stroke. The datum was set at the moment the piston came in contact with the loose material, which was defined as zero time. This occurred when the material had its initial density, ρ_0, prior to compaction (Fig. 3-5).

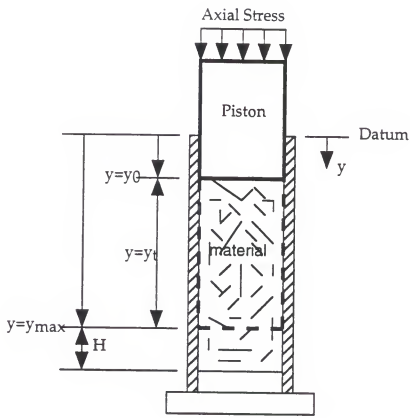

Fig. 3-5. Diagram and definitions of material deformation.

Piston displacement was used to determine the material deformation and density during compression. The second quantity was the manner in which the applied axial load

(force) varied with time. This quantity was required to determine applied stress at any time during the piston compression stroke.

Piston displacement was measured using a DC-DT displacement transducer from Hewlett Packard with a maximum stroke of 15 cm. It was not possible for practical reasons to directly connect the transducer to the piston. Hence, an indirect arrangement was adopted. An inextendible cord was attached to the transducer and connected to the piston head through two overhead small pulleys which were fixed vertically above the DC-DT and the piston head, respectively. A small weight was placed between the cord and transducer to ensure stable movement. Fig. (3-6) shows a general view of the compression setup and equipment. To get the maximum possible accuracy of the displacement data, the transducer was calibrated on a daily basis. A typical calibration curve of the displacement transducer is shown in Fig. (3-7).

A load cell was designed and manufactured in the Agricultural and Biological Engineering Department at the University of Florida with maximum capacity of 130 kN (30,000 lbf). It was calibrated in the laboratories of the Department of Materials Science and Engineering. The calibration curve of the load cell is shown in Fig. (3-8).

Preliminary Experiments

As stated previously, no literature was found in which these particular materials were processed into wafers. Therefore, preliminary experiments were required and conducted in order to determine suitable values or ranges of the variables investigated. This applied in particular to holed time, stress, MC, and charge. Accordingly, three

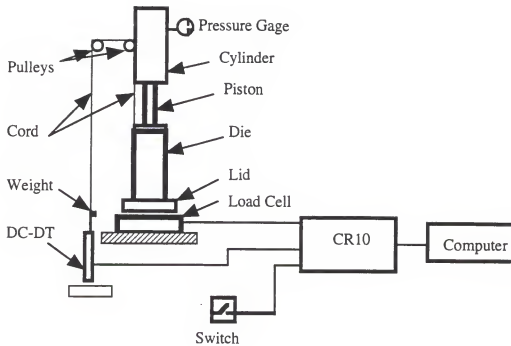

Fig. 3-6. A general diagram of compression setup and arrangement of equipment.

levels of hold time were chosen. A 15-second and 5-second hold times were deemed reasonable maximum and minimum. The third level, which was selected in between, was set at 10 seconds.

The stress levels applied on the material varied with die diameter due to the limited maximum capacity of the press. The arrangement shown in Table (3-1) was chosen. Similarly, the charge was proportional to the size (diameter) of compression cylinder. Table (3-2) lists the quantities used for each diameter. It is noteworthy here that a compromise between adequate machine capacity and wafer quality was sought.

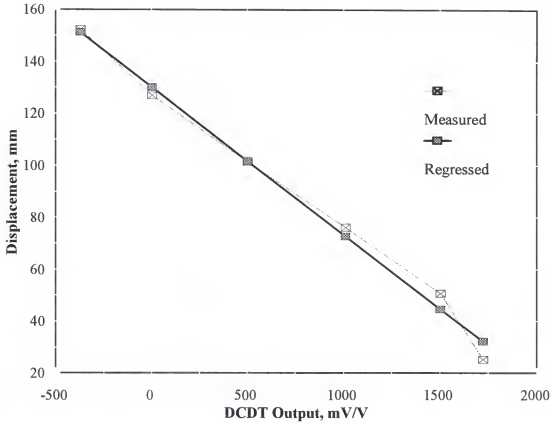

Fig. 3-7. A typical calibration curve of the displacement transducer (DC-DT).

Table 3-1. Maximum stress levels applied in different compression dies.

Die diameter (mm)	Maximum stress applied (MPa)			
40.0	17.0	24.0	37.0	58.0
50.0	17.0	24.0	37.0	
63.0	17.0	24.0		
76.0	17.0			

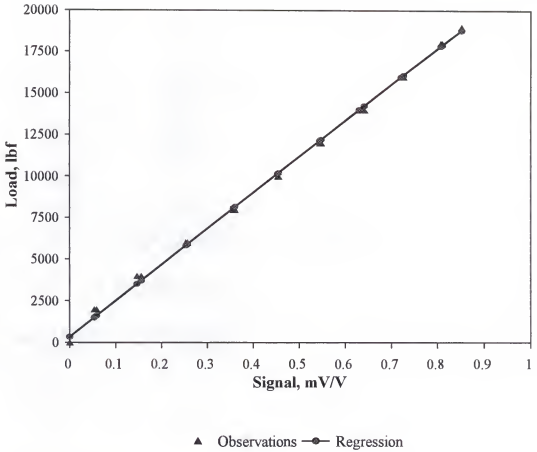

Fig. 3-8. The calibration curve of the load cell.

Table (3-2). Material weight (charge) used in the different compression dies.

Die Diameter (mm)	Wafer weight (charge) (gm)
40.0	12.0
50.0	15.0
63.0	20.0
76.0	27.0

It was realized from the preliminary work that the MC of stored material was too low to wafer especially at lower pressures (larger diameters). Thus, the material had to be re-wetted to raise its moisture content to acceptable levels. To do so, a given weight of material was placed in plastic containers, sprayed with a predetermined amount of water and tightly covered.

To ensure uniform moisture distribution, containers were left to set under ambient conditions for 48 to 72 hours during which the material was mixed 2 to 3 times. The material MC was determined by drying the material in an oven at 103 C for 24 hours according to the ASAE standards S358.2 (ASAE, 1996). In this work, the material moisture at the time of compression ranged from 13 to 19% (w.b.). At higher MC, it was very hard to make a stable product and wafers disintegrated immediately upon removal from the die.

Processing Material into Wafers

Once the preliminary work was completed, compression and data collection phases were started. The experimental design was arranged such that at each of the four stress level, the three hold times were used for each die diameter. This combination resulted in 30 different treatments for each material. For each treatment, 15 wafers (replicates) were made from the same container at a given MC. In each replicate, a predetermined amount (charge) was weighed on a digital balance, hand-fed into the die, and prepared for pressing by placing the die under the piston and on top of the load cell.

The piston extended into the die at a given rate until it reached a designated maximum pressure set by adjusting the relief valve on the press. The material was held at that pressure for the duration of hold time, which was measured by a stop watch and the wafer was finally ejected as described above. Approximately 5 minutes were allowed between consecutive replicates to prepare for the next run and readjust the load cell and DC-DT to the zero position.

Upon ejection, each wafer was immediately weighed, and its dimensions, namely, thickness and diameter, were measured. Wafers were then placed in plastic freezer bags and stored under ambient conditions. Further, for each replicate, piston displacement and load applied onto the loose material were measured every second. This was achieved by employing a data logger model CR10 connected to both the DC-DT transducer and load cell as well as to a laptop computer. A switch was attached to the data logger to control data flow from its memory into the computer and thus avoid irrelevant data during idling.

CHAPTER 4
FORMATION CHARACTERISTICS OF WAFERS

Introduction

After wafers are made to be used as an energy source, there are two fundamental quality aspects of the product that should be investigated. The first is their handling characteristics and the second is their characteristics as fuel. The first aspect will be considered in this chapter and the next while the second aspect will be discussed in chapter 6. In this chapter, the characteristics of wafer formation during compaction including reduction in raw material bulk density and volume, the pressure- or stress-density relationship and compaction energy requirement are addressed. Pressure and energy are important considerations in the functional and structural design of compaction machines.

One of the major justifications of biomass compaction is the reduction in volume of the bulky material, which is associated with a corresponding increase in density. Density was the quantity of interest since it is one of the most important physical characteristics of wafers. Further, it is directly involved, as will be shown

later on, in expressing wafer stability and determining the handling characteristics of the final product.

It is important at this point to clarify the terminology used in association with density. The term apparent density, also known as actual or unit density and symbolized as ρ, refers to the density of an individual wafer. For simplicity, the term density will most often be used to denote ρ. Several specific cases of the product apparent density exist. The final or relaxed apparent density, ρ_f, is the density of a wafer 24 hours after formation. In this time period, the wafer was left to expand and relax freely. Immediate density, ρ_m, is the wafer density measured immediately after the wafer was ejected from the chamber while the initial density, ρ_0, is defined as the material density in the chamber prior to compaction.

The term instantaneous density, ρ_i, was used to describe the apparent density of material (charge) in the die at any instant during the compression stroke. In contrast to material apparent density, bulk density of the final product may be defined as the overall density of many pieces (wafers) piled together including the pore space.

All density measurements in this work were based on material weight to volume ratio. Weight was determined by measurement and volume was calculated from the wafer thickness and cross-sectional area. The wafer cross-sectional area was considered constant for each wafer by assuming its diameter was equal to the internal diameter of the die in which the wafer was made. The justification of this assumption will be made clear in the following chapter.

Results and Discussion

Bulk Density and Volume Reduction

In such applications as wafering, bulk density is more important than unit density because it is a more accurate indicator of the savings in transportation and storage space realized by compaction (Miles, 1995; Beck and Halligan, 1980). However, the wafer unit density and its shape are the major factors in determining the product bulk density. Data for elephantgrass showed that material immediate and final density were, respectively, 8 to 12 and 6 to 9 times its initial density and the corresponding figures for energycane were 7 to 11 and 4 to 9, respectively, depending on die size and stress level. Smaller dies and higher pressures produced the higher densities and vice versa.

It was reported that for biomass wafers, a factor of two between unit and bulk density was generally appropriate (Erikson and Prior, 1990). Applying this figure to the final density data showed that elephantgrass bulk density was increased by a factor of 3 to 4.5 while that of energycane was increased by a factor of 2 to 4.5. These figures were in or beyond the range required for transportation vehicles to be loaded to their full capacity as was reported by Smith et al. (1977).

It should be emphasized, however, that the figures above were based on a comparison between the material immediate and final density on the one hand and initial density on the other. A more realistic comparison would be based on the density

of loose material in its free unconsolidated state. Prior to filling in the chamber, the material occupied roughly twice the volume of uncompressed material in the die. Accordingly, the bulk density of compressed elephantgrass and energycane was, respectively, 6 to 9 and 4 to 9 times that of raw material. In terms of volume and based on the product final volume (after expansion), data indicated that, in the two smaller chambers (40- and 50-mm), a volume reduction in the range of 6.5:1 to 10:1 was achieved as compared to the material volume in the die prior to compression. Relative to the loose material, these ratios could be at least twice as much.

Whenever utilization of bulky biomass materials is considered, transportation and storage costs, called handling costs, of such materials come into play as major factors. Clearly, these costs are determined primarily by the material volume and bulk density. Furthermore, the importance of increasing material bulk density and reducing its volume may be amplified in light of the fact that several advantages of biomass materials such as being renewable, better distributed throughout the world, and pollution potential are hard or, at least, controversial to quantify. Unfortunately, these advantages are usually underestimated and in many cases become only minor considerations. This results in placing much higher value on the direct costs associated with biomass material handling. Therefore, material volume and bulk density are of utmost importance in the economic feasibility of using biomass materials for virtually any purpose including using them as fuel.

Stress-Deformation Relationship

The material was compressed by applying load onto the loose material in the die to a maximum value, which was held for the duration of dwell time. The stress was determined by dividing the load by the cross-sectional area of the die. In this chapter, the term stress refers to the stress at any instant during the compression stroke with values ranging from zero to a maximum value, P_{max}. Material deformation is meant to refer to the change in material height in the die due to the applied stress. The manner in

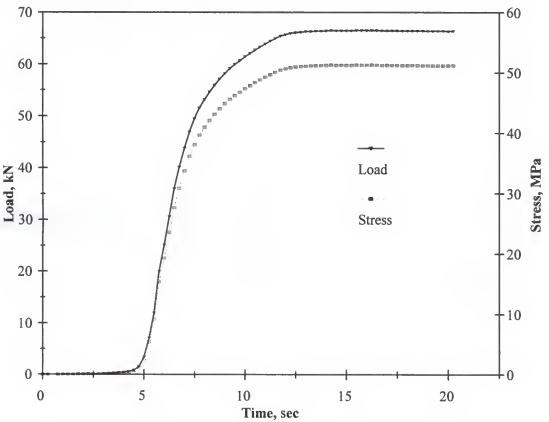

Fig. 4-1. Change in applied axial load and stress with time during compression stroke.

which the load and stress applied varied with time is shown in Fig. (4-1) and the material deformation with time is shown Fig. (4-2). Notice that compression rate may be determined from the slope of the deformation-time curve.

It was noted that the material deformed approximately at a constant rate in the early stage then slowed down and eventually reached a steady-state value implying that

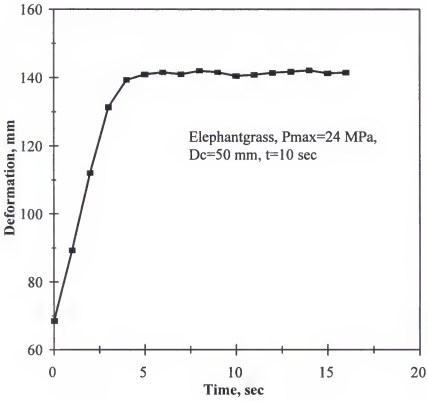

Fig. 4-2. Material deformation response with time under axial stress.

the material reached its ultimate deformation under the applied stress. A typical stress-deformation curve representing both materials is shown in Fig. (4-3). It is clear

from the curve that the relationship assumed the following form

$$\sigma = \alpha 10^{\beta y} \tag{4-1}$$

where α and β are empirical constants

y is the material deformation

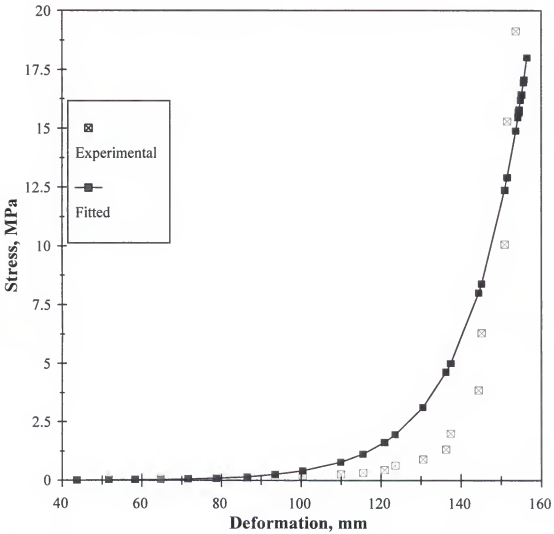

Fig. 4-3. A typical stress-deformation relationship for elephantgrass and energycane.

It can be seen from the curve that in the initial stage of compression, the material resistance was very small indicating a behavior of a highly compressible material. In this stage, the load had to overcome the force of bringing material particles closer together by merely reducing the pore space. This was mainly achieved by forcing air out from the material pore space.

Advancing the piston further in the compression stroke caused gradual increases in load required to effect mechanical changes in material particles in the form of bending and crushing. Toward the end of the compression stroke, the curve shows a rapid increase in load after a certain displacement is exceeded, indicating a response similar to that of an incompressible material. In this last region and beyond, tremendous loads are required to achieve only slight increases in material deformation. This sharp rise in stress level as the deformation approached zero indicated that the material was compressed as much as was apparently possible by the load (Fig. 4-2).

Like the vast majority of biological materials, the nonlinear nature of the stress-deformation relationship of elephantgrass and energycane is evident. This might provide an additional example on the necessity of modeling agricultural materials as nonlinear when it comes to their stress-strain relationship. It may be added here that although $R_d^2 > 0.9$, the fitted curve (Fig. 4-3) can serve only as a rough qualitative assessment of the nature of the stress-deformation relationship. A similar argument applies for the stress-specific volume fit where an attempt to improve the fit will be carried out later in this chapter. Only simple adjustments are required over the stress-specific volume improved fit to adapt it to the stress-deformation relationship.

Stress-Density Relationship

The design of suitable wafering equipment requires a knowledge of the stress (pressure) and load required to obtain a desired degree of compression, which necessitates a relation to predict the stress in terms of product density. Therefore, the relationship between the pressure and the instantaneous density of biomass materials under compression was among the most intensely investigated aspects of biomass densification. The material instantaneous density at any point was calculated using the material instantaneous thickness from the displacement transducer output in addition to its weight and diameter.

In order to get a mathematical stress-density relationship, the experimental data points were plotted and curves were fitted to them. The computer graphics software CricketGraph was used for all curve fittings performed in this study. A good representation of the results for both materials and all cases was given by the equation

$$\sigma = a10^{(b\rho_i)} \tag{4-2}$$

where σ is the stress on the material in the die during compression (MPa)

a and b are parameters

ρ_i is the instantaneous density of material in the die during compression

It can be seen from Eqn. (4-2) that a knowledge of the satisfactory range of product density determines the level of stress required. The latter has profound consequences on the energy required, compaction machine design and the optimization of the process.

Notice that the arguments and comments presented for the stress-deformation relationship as to what happens during the compression stroke apply to the σ-ρ_i as well. Typical curves for both materials are shown in Figs. (4-4) and (4-5). Notice also that the values of ρ_i range from ρ_0 to ρ_m, that is,

$$\rho_0 \preceq \rho_i \preceq \rho_m$$

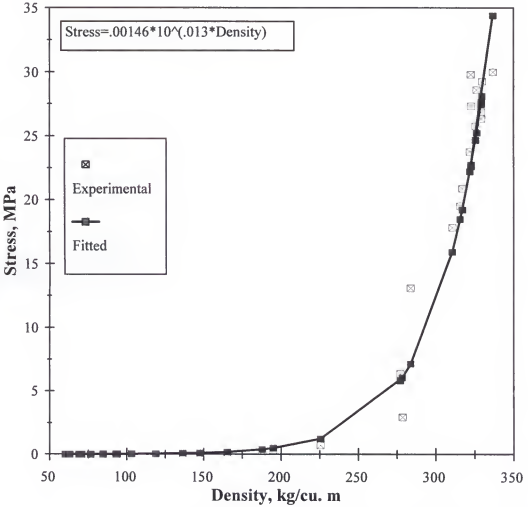

Fig. 4-4. Variation of material instantaneous density with the applied axial stress for elephantgrass.

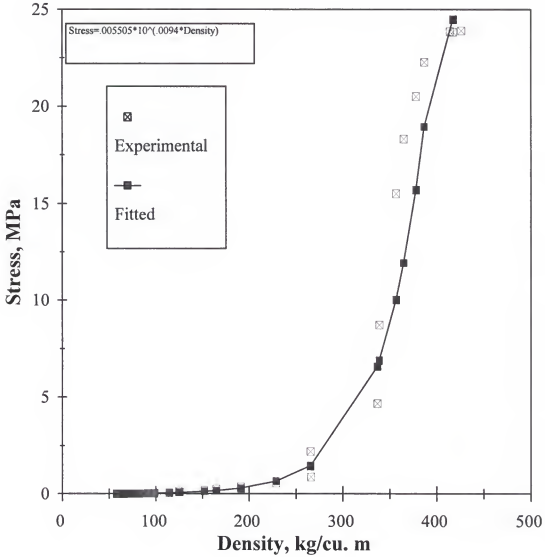

Fig. 4-5. Variation of material instantaneous density with applied axial stress for energycane.

Eqn. (4-2) was clearly of exponential nature and represented the best fit to the experimental data points since all correlation coefficients for the fitted curves were in excess of 0.90. When plotted on a semi-log paper, the equation gives a straight line

as shown in Fig. (4-6). This can be demonstrated by taking the logarithm of both sides of the equation, which yields

$$\log\sigma = \log a + b\rho_t \tag{4-3}$$

where the constants Log (a) and b are the intercept and slope, respectively.

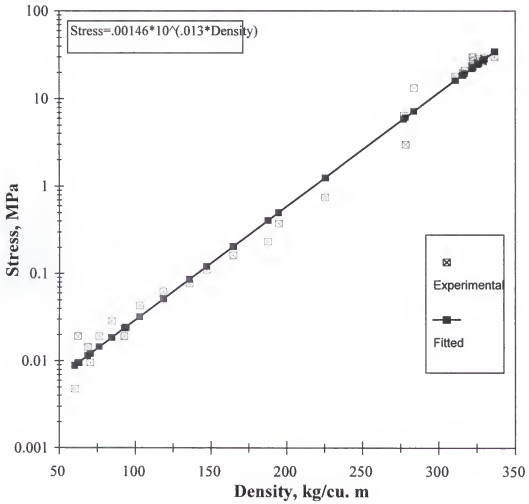

Fig. 4-6. Material stress-density relationship on semi-logarithmic scale.

Eqn. (4-3) states that the material density in the die was linear with the logarithm of the pressure applied. Careful inspection of Eqn. (4-3) revealed that it had some limitations on its use due to its purely empirical nature (Bilanski et al., 1985). The model equation (Eqn. 4-3) could be rearranged to express ρ_i in terms of σ, i.e.,

$$\rho_i = b_1 \log(\frac{\sigma}{a}) \qquad (4\text{-}4)$$

where b_1 is the reciprocal of b.

In fact, Eqn. (4-4) is precisely the same formula proposed by Butler and McColly (1959) for the compaction of hay in a closed-end die (Eqn. 2-1). This form of the equation shows that it fails to define properly the value of ρ_i at the static condition where σ approaches zero. In other words, as σ becomes very small, the equation gives unrealistic estimates of ρ_i in the sense that it yields negative values of ρ_i while in reality it should be equal to ρ_0. Furthermore, the equation indicates that, in theory, the density will increase indefinitely with increasing stress. In reality, the material density will reach an ultimate value beyond which essentially no increases will be realized as pointed out in the previous section for deformation since density is directly proportional to deformation.

The limitations mentioned above necessitate the use of this equation within the ranges of density, stress and other conditions used in this study. To alleviate this drawback, a dimensionless density term, u, defined in a model equation proposed by Bilanski et al. (1984) was adopted and applied to the experimental data of this study.

This model equation was developed for the compression of alfalfa and grass in a closed-end die and was based partially on an analysis of the mechanics of material compaction. The equation was introduced in Ch.2 (Eqn. 2-3) where u was defined as

$$u=\frac{\rho_{max}-\rho_i}{\rho_{max}-\rho_0}$$

where ρ_{max} is the maximum density the material attained under a given P_{max}. Notice that the value of the non-dimensional density term, u, ranges from zero to one, that is,

$$0\le u\le 1$$

The experimental data of u were plotted against those of stress and curves were fitted to the data using a curve-fitting computer software. The best fit to the data was of the form

$$u=c_0-c_1\log(\sigma) \qquad (4\text{-}5)$$

where c_0 and c_1 are constants both greater than zero. For illustration purposes, two representative examples of the results of fitting Eqn. (4-5) to the data are shown in Fig. (4-7) and Fig. (4-8) for the two materials.

Examining the curves clearly shows that although this model equation is still empirical, it has successfully overcome the two shortcomings of the previous proposed model (Eqn. 4-4) mentioned above. It can be seen from the figures that as the stress

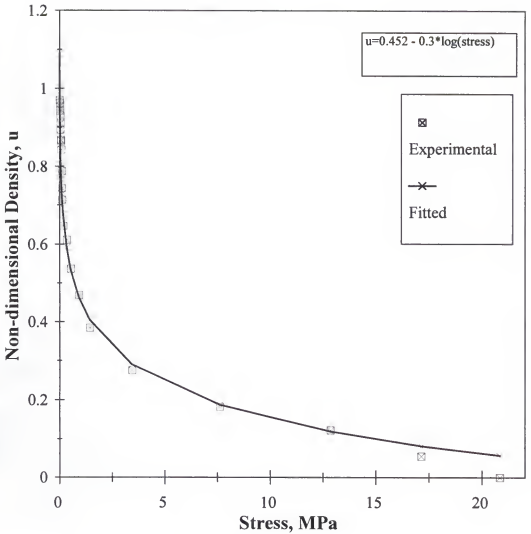

Fig. 4-7. Relationship between the applied axial stress and the modified non-dimensional density of elephantgrass.

level approaches zero, which occurs at the start of compression stroke, the dimensionless density, u, approaches unity, that is,

$$u = \frac{\rho_{max} - \rho_i}{\rho_{max} - \rho_0} = 1.0$$

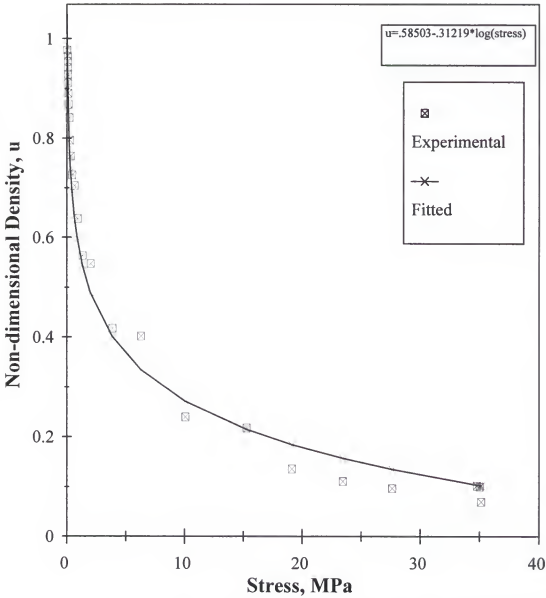

Fig. 4-8. Relationship between the applied axial stress and modified non-dimensional density og energycane.

The last expression implies that $\rho_i = \rho_0$, which indicates that the static condition has been satisfied. On the other hand, it is noted that as the stress level becomes very high at the end of compression stroke, the value of u approaches zero, i.e.,

$$u = \frac{\rho_{max} - \rho_i}{\rho_{max} - \rho_0} = 0$$

which clearly implies that $\rho_i = \rho_{max}$, which is the maximum density the material can possibly attain under the applied maximum stress, P_{max}.

Many researchers reported the same general relationship between axial stress applied and material instantaneous density, that is, an exponential or logarithmic relationship. Chapter 2 on literature review presented some examples on this point. This may serve as an indication that elephantgrass and energycane share common behavior with and respond in a similar fashion to other biomass materials when compressed under uniaxial stress in a closed-end die.

A value of special interest in this regard is the density of the wafer at the end of the compression stroke when the stress value is at its peak, i.e, $\sigma = P_{max}$. At this point, the product density is ρ_{max}. In this study, the actual ρ_{max} of wafers was not measured. Instead the wafer immediate density, ρ_{max}, was the highest product density measured. The following section will cover this important wafer characteristic in some detail.

Wafer Immediate (maximum) Density

In this work and according to the definitions above (see Eqn. 4-3), it may be stated that

$$\rho_m \approx \rho_{max}$$

The value of ρ_m represents approximately the maximum density the material possessed at the end of compression stroke under a given applied maximum stress. It will be shown in the next chapter that ρ_m is a primary factor in determining one of the most important wafer characteristics, namely, the product final density, ρ_f. The relationship between ρ_m and maximum stress, P_{max}, is shown in Figs. (4-9) and (4-10) for the two materials with die diameter, D_c, as a parameter. It is clearly illustrated that higher stress levels as well as smaller dies resulted in wafers with higher ρ_m in all compression cylinders. A detailed discussion of the influence of wafering conditions including P_{max} and D_c on wafer density is presented in the next chapter.

It was clear though that ρ_m was not a function of P_{max} and D_c only, rather, it depended on other variables. According to the physics of the compaction process, the relevant independent variables included the following process and material variables: hold time, t_h, maximum stress, P_{max}, die diameter, D_c, material moisture, MC, wafer relevant independent variables included the following process and material variables: hold time, t_h, maximum stress, P_{max}, die diameter, D_c, material moisture, MC, wafer charge (weight), W, and material initial density, ρ_0. The functional relationship between the dependent variable ρ_m and independent variables for both materials was

$$\rho_m = f(t_h, P_{max}, D_c, MC, W, \rho_i)$$

A first-order linear regression model of the following form was proposed

$$\rho_m = \beta_0 + \beta_1 t_h + \beta_2 P_{max} + \beta_3 D_c + \beta_4 MC + \beta_5 W + \beta_6 \rho_0 + \varepsilon \qquad (4\text{-}6)$$

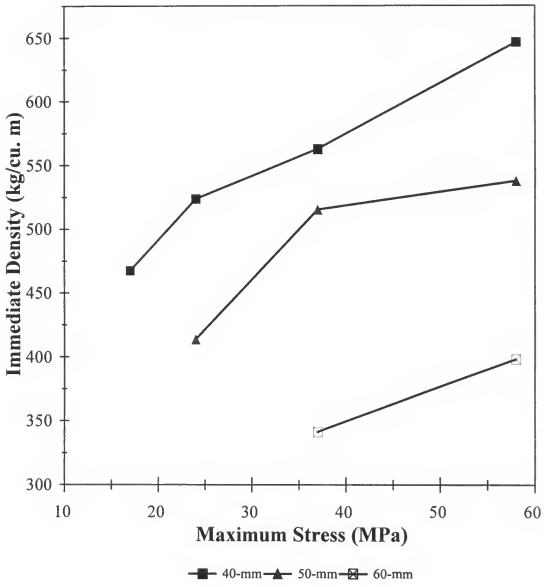

Fig. 4-9. Influence of maximum compression stress on elephantgrass immediate density.

where ε designates an error term, and

β_i are parameters, i=1,2,...,6.

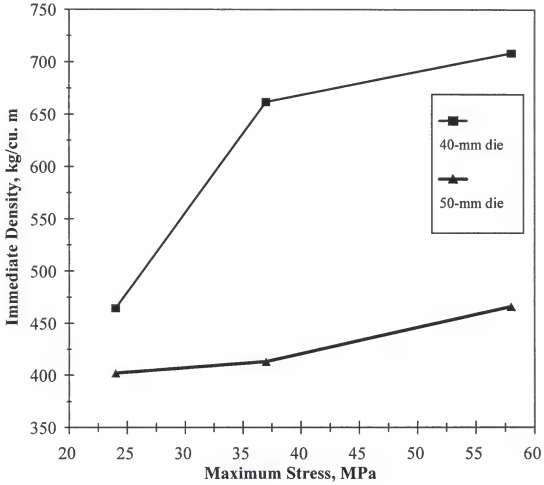

Fig. 4-10. Influence of maximum applied stress on immediate density of energycane.

The statistical software package SAS was used to develop the prediction equations. For elephantgrass, the SAS output showed that all parameters, β_i, were highly significant at the 0.05 level except that attached to the weight. Therefore, the variable representing the wafer weight was dropped out. Thus, the prediction equation was the following:

$$\rho_m = 521.1 + 1.87t_h + (3.3e-6)P_{\max} - 2886.0D_c - 7.6MC + 3.06\rho_0 \qquad (4\text{-}7)$$

The values of ρ_m predicted by Eqn. (4-7) above vs. measured values are shown in Fig. (4-11) below.

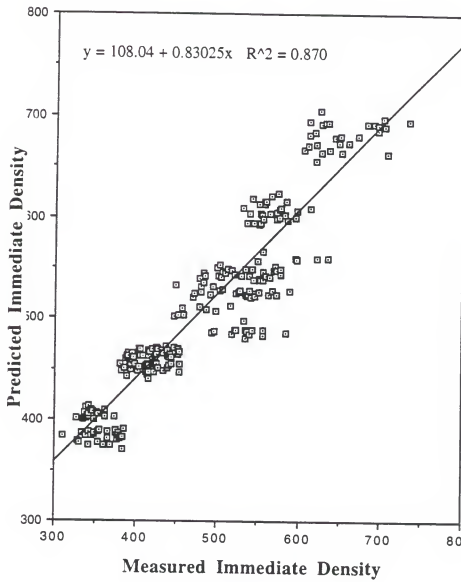

Fig. 4-11. Predicted versus measured values of elephantgrass immediate density.

As for energycane, it turned out that all parameters, β_i, were highly significant at the 0.05 level and, therefore, the prediction equation included all variables. The prediction equation was

$$\rho_m = 1187.3 - 1.38t_h + (5.2e-6)P_{\max} - 14495.0D_c - 25.9MC + 18.8W + 0.39\rho_0 \qquad (4\text{-}8)$$

Fig. (4-12) shows the predicted vs. measured values of ρ_m. The last two figures show that approximately 90% of the variation in ρ_m is attributed to those variables.

From equations (4-7) and (4-8), it is evident that higher ρ_0 results in higher ρ_m for both materials. It was noticed that material initial density in smaller dies was higher than that in larger ones, which may be one reason why smaller dies produced wafers with higher ρ_m. It may also be noted that as far as P_{max} and D_c are concerned, the prediction equations for both materials are consistent with the discussions presented earlier. This is demonstrated by the signs attached to the parameters of these variables.

The influence of dwell time here deserves some clarification. Although it will be shown that longer hold time had generally weak positive influence on wafer final density by effecting less wafer post-compression expansion, it seems here that it caused larger spring back of energycane wafers at the instant of unloading due to their high proportion of resilient stems compared to the leafy elephantgrass. A detailed discussion of the influence of P_{max}, D_c, W, and t_h on wafer density is presented in the next chapter in the section on wafer stability.

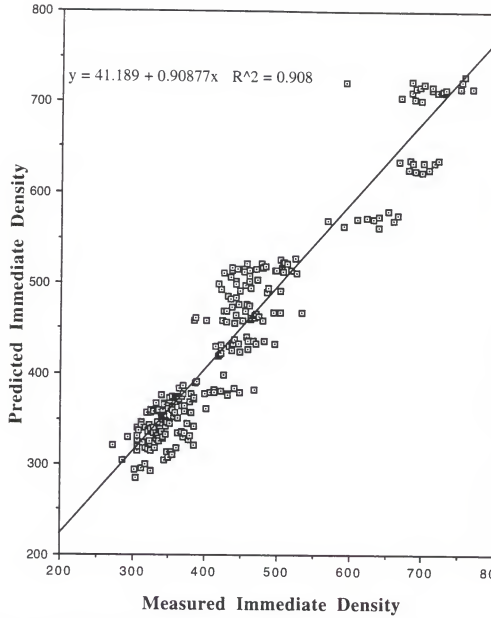

Fig. 4-12. Predicted versus measured values of energycane immediate density.

Energy Requirement

In deciding whether compressing the material into wafers is practical under given circumstances, it is essential to consider the energy required for compaction.

Along with other aspects of densification, a knowledge of the energy required allows for the design of better compaction processes.

The work (energy), E, required for material compression is given by

$$E=\int F dy \tag{4-9}$$

where F is the applied force, and

dy is the change in material thickness in the die

For a die with a constant cross-sectional area, A, as is the case in this study, Eqn. (4-9) may be rewritten as

$$E=A\int \sigma dy \tag{4-10}$$

where σ is the applied axial stress. Thus, a knowledge of the load or stress applied and the change in material thickness during compression is necessary and sufficient to determine the energy required for compaction. In this study, Eqn. (4-9) will be used for energy calculations utilizing the force-displacement curves. The energy required can be interpreted as the area under such curves, which is evaluated by performing the integral shown in Eqn. (4-9) between any two points during the compression stroke.

The value of most interest is the total energy consumed during compression of a single wafer. Thus, the history of the load applied throughout the process and the total change in material thickness between the point of initial thickness ($y=y_0$ and $F=0$) and the minimum thickness ($y=y_{max}$ and $F=F_{max}$) are required (see Fig. 3-1). The mathematical computer software was utilized to fit a curve the force-deformation data

points. The force-deformation relationship assumed an exponential form and the best fit to the data was

$$F=B_0 10^{B_1 y} \tag{4-11}$$

where y is the displacement (deformation)

B_0 and B_1 are parameters.

The identical form of the force-deformation and stress-deformation relationships (Eqns. 4-1 and 4-11) is expected because they are related by a constant factor, which is the cross-sectional area of the compression cylinder. Table (4-1) lists the values of the constants B_0 and B_1 under different conditions for both materials.

The expression for F from Eqn. (4-11) was substituted in Eqn. (4-9) to obtain

$$E=\int B_0 10^{B_1 y} dy \tag{4-12}$$

The computer software Mathcad was used to perform all the integrals. The results of energy requirement per wafer for all cases are shown in Table (4-2) for both materials. These values were converted to specific energy values (MJ/ton), also shown in the table, based on the weight of each wafer.

It was found that the energy required for the compression of either material covered a wide range from 11 to 50 MJ/ton in direct proportionality with stress level applied and die diameter. This amount of energy was only a small fraction of the

Table (4-1). Values of B_0 and B_1 in the force-deformation relationship for the two materials.

Dc (mm)	Pmax (MPa)	Material			
		Elephantgrass		Energycane	
		B_0x10^5	B_1x100	B_0x10^5	B_1x100
40.0	58.0	0.043	5.05	236.20	2.62
	37.0	0.035	5.11	6.60	3.42
	24.0	0.830	4.01	7.66	3.40
	17.0	0.297	4.30	----	-----
50.0	37.0	0.00033	7.29	1.90	4.59
	24.0	0.242	5.11	0.66	4.87
	17.0	1.41	4.40	73.30	3.27
63.0	24.0	0.028	5.68	3.04	4.31
	17.0	0.091	5.36	78.50	3.12
76.0	17.0	2.81	4.44	$3.44x10^{-5}$	8.32

material's calorific value and ranged from 0.1% to 0.3% of their energy content. This compares very favorably with many other biomass materials, which required 5 to 10% of their energy content for compaction (Beck and Halligan, 1980).

Faborode and O'Callaghan (1987) studying straw claimed that errors were introduced when the compaction energy was simply determined from the area under the force-deformation curve. They defined a "true" energy term, E_r, as

Table (4-2). Energy requirement for the compaction of elephantgrass and energycane under different wafering conditions.

D_c (mm)	P_{max} (MPa)	Energy/Wafer (kJ) EG[a]	EC[b]	Specific Energy (MJ/ton) EG	EC
40.0	58.0	512	650	42.65	54.15
	37.0	370	375	30.82	31.24
	24.0	240	250	19.99	20.83
	17.0	185	-----	15.41	-----
50.0	37.0	318	395	21.20	26.33
	24.0	280	380	18.67	25.33
	17.0	220	305	14.67	20.33
63.0	24.0	490	230	24.50	11.50
	17.0	430	214	21.50	10.70
76.0	17.0	755	370	27.96	13.70

[a] EG is an abbreviation of elephantgrass
[b] EC is an abbreviation of energycane

$$E_T = EF_{te}$$

where F_{te} is a true energy factor (for straw, $1 < F_{te} < 2$).

The authors justified the introduction of F_{te} by running repeated compression tests as a sequence of stress application. They indicated that the material expanded rapidly and additional energy was required in the next sequence to bring the material

back to the point of the previous one. Nonetheless, as far as this study is concerned, if it is assumed that F_{te} for elephantgrass and energycane is in this same range as straw, the energy required for material compression will still be a small fraction less than 1% of the material energy content.

Close examination of the data revealed that actual loads (stresses) were slightly less than proposed values. This is not expected to introduce any serious errors in energy calculations because most of the energy was consumed by the time the applied load approached its proposed maximum value. Increasing the maximum load at the apex of the force-displacement curve would result in only slight increases in energy expended due to the minimal deformations taking place at that point as mentioned previously.

Data in Table (4-2) indicated that in any given compression cylinder, higher loads (stresses) were associated with higher energy requirement for both materials. This trend is shown in Fig. (4-13) for elephantgrass. This result is a direct outcome of the definition of energy expended as presented in Eqn. (4-9). Further, the data showed that for the same stress level, significantly higher energy was generally required in larger dies than in smaller ones as shown in Fig. (4-14). This was principally due to the higher load required to effect a given stress in larger chambers because of their larger cross-sectional area. Moreover, the larger charge in larger cylinders might have involved more friction among material particles and with die surfaces so that it absorbed more energy.

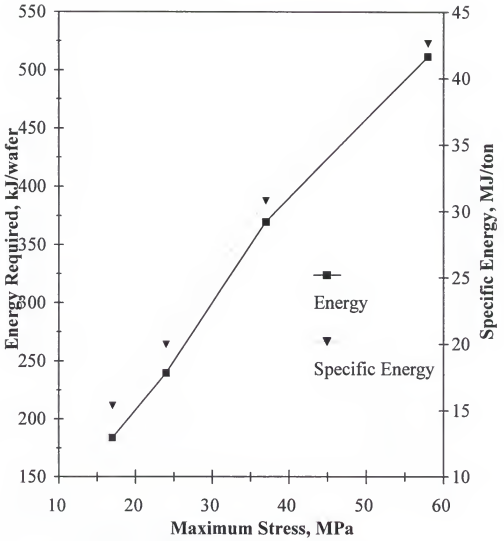

Fig. 4-13. Compaction energy as a function of the applied maximum stress for elephantgrass in the 40-mm die.

As higher stresses were normally associated with a higher product density as was shown in the previous section (Eqns. 4-4 and 4-5), it may be concluded that denser wafers, which were usually of better quality, required more energy to make. However, since it is desirable in any efficient compaction process to minimize the energy required

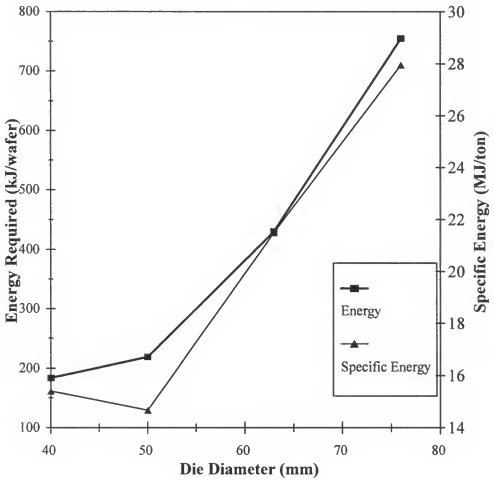

Fig. 4-14. Compaction energy required as a function of die size for elephantgrass in the 40-mm die.

and still maintain acceptable wafer quality in stability and handling, a compromise must be sought between the energy consumed and acceptable product density and consequently quality.

A different and useful perspective of the compaction energy required that is worth a comment may be realized by considering the applied stress and material specific volume, v. Obviously, in contrast to the force-deformation approach, this

aspect involves a knowledge of the applied stress and material specific volume, which is the reciprocal of material density.

Once the area under the σ-υ curve is calculated by integration, for instance, it provides a value for the specific energy required, which is an apparent advantage. This is because it saves the effort needed to convert the compaction energy per wafer, which is the outcome of the force-deformation approach, to specific energy values. Specific energy is the most common criterion utilized to evaluate biomass densification from an energy viewpoint. A typical example with an exponential fit of the σ-υ curve from this study is shown in Fig. (4-15).

As pointed out for the force-deformation curve, the fit for the σ-υ is intended to serve only as an approximate qualitative description of the relationship. An attempt was made to improve the fit. The form of the improved fit for the σ-υ relationship included two exponential terms. In symbolic form, it was

$$\sigma = A[\exp(-\alpha\upsilon)] + B[\exp(-\beta\upsilon)] \qquad (4\text{-}13)$$

where A, B, α, and β are parameters. Fig. (4-16) shows an example of the fitted points according to Eqn. (4-13). It may be clearly seen that significant improvement was achieved using Eqn. (4-13) in fitting the data. A form identical to Eqn. (4-13) with minor modifications can be used to improve the fit for the force-deformation data.

As far as energy requirement of handling and processing (densification) of biomass materials is concerned, it should be born in mind that although compaction energy is a major consideration, it is only one of several components. In order to carry

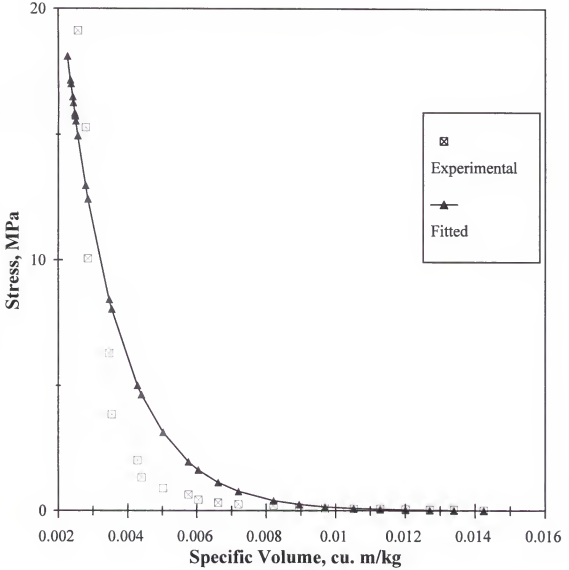

Fig. 4-15. A representative example of axial stress-specific volume relationship for elephantgrass and energycane.

out a comprehensive assessment of the total energy involved in the conversion of biomass to fuel, other energy components must be addressed. In this study, no attempt was made to estimate the other components. Nonetheless, it may be useful to point out that other major energy components include the energy required for drying, crushing

and grinding, and harvesting and transportation of biomass. The determination of total energy required becomes a necessity if an overall economical appraisal of a potential project or business based on this concept is pursued.

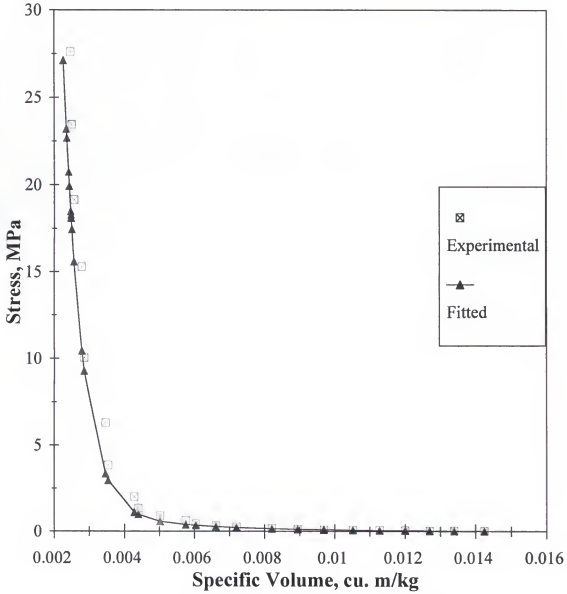

Fig. 4-16. Stress-specific volume data with a curve fitted according to Eqn. (4-13).

CHAPTER 5
WAFER QUALITY

Introduction

Between the time of formation and the time of end use, wafers experience expansion in dimensions and are subject to damage during handling and transportation. In addition to expansion, fine-producing forces, mainly impact and friction (shearing), cause a reduction in wafer weight and change of its size and possibly shape. Thus, the production of wafers of acceptable quality is a major concern to those involved in the wafering and handling equipment as well as the end users.

Wafer quality as used in this text is intended to serve as a measure of the handling characteristics of wafers. It is evaluated by existing test procedures developed by the ASAE. These standard tests provide the means by which the durability and stability of wafers are determined. Many factors play a role in influencing the quality of wafers produced. These factors include raw material properties such as forage species, source of forage, particle size, material moisture content and material temperature in addition to the wafering conditions such as stress and die size. The manner in which

these factors and their interactions affect the quality of wafers produced is quite involved and complex.

In this study, an attempt was made to achieve as much uniformity as possible and many of these factors were assumed to be fixed by virtue of the experimental design. For example, the material was harvested from the same plot at almost the same time, stored under the same conditions, cut to the same nominal size and brought to the narrowest possible range of moisture. Consequently, in this chapter, only three of these factors were considered, namely, maximum pressure, P_{max}, hold (dwell) time, t_h, and diameter of compression die (chamber), D_c.

Due to the limited control over some of the variables such as the variation in material moisture, MC and weight beyond the desirable pre-specified ranges in addition to other factors believed to be relevant to wafer quality, the following analyses include those additional factors.

Materials and Methods

Wafer quality is expressed in terms of two criteria: stability and durability. Stability of a wafer can be defined as the ability of a wafer to restrain from changes in its initial physical dimensions (Gustafson and Kjelgaard, 1963). Wafer stability for both materials was determined by observing their post-compression expansion. The changes in product dimensions in the axial and lateral directions (thickness and diameter) were

recorded over a 24-hour observation period as shown in Table (5-1). The zero time was defined as the time at which the wafer was ejected.

Table (5-1). Scheme of measuring wafer expansion during the observation period.

Dimension Measured	Time After Wafer Formation (hr)
Axial, Radial	0.5
Axial, Radial	1.0
Axial, Radial	3.0
Axial, Radial	6.0
Axial, Radial	10.0
Axial, Radial	15.0
Axial, Radial	24.0

Wafer expansion lead to increases in its dimensions accompanied by corresponding reductions in density. Since the wafer final density, ρ_f, is the characteristic of greatest practical interest in relation to stability (O'Dougherty and Wheeler, 1984) and is directly proportional to changes in product physical dimensions, it was the criterion used to express and evaluate wafer stability.

The ultimate goal of wafering is the production of durable wafers because durability is the fundamental criterion in defining wafer quality. The durability of a wafer may be defined as the ability of the wafer to withstand the rigors of handling. It

is evaluated by the durability rating (%), which is basically the percent weight retained by the wafer after tumbling. During the test, wafers are subjected to a treatment simulating the abuse which they might experience in normal handling operations.

Wafer durability was measured by utilizing a shop-built tumbler, shown in Fig. (5-1). The tumbler was fabricated for this purpose according to the ASAE standards S269.4 (ASAE, 1996). A sample of 10 wafers of each treatment was tumbled 24 hours after they were formed (ejected from the die) and their durability rating was determined. Table (5-2) shows a worked-out example of the standard procedure followed to determine the durability rating of wafers according to the recommendations of the ASAE. In this study, a criterion was set such that a durability rating$\geq$70% was rated acceptable, otherwise the durability was rated as poor (Reece, 1965).

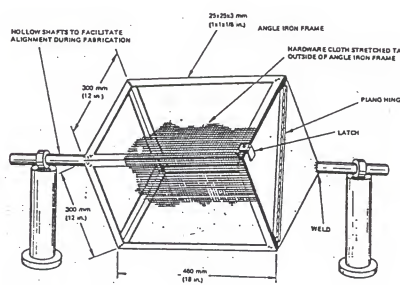

Fig. 5-1. Durability tester (tumbler) for wafers. (Source: ASAE Standards, 1995, p. 444).

Table (5-2). The recommended worksheet used to calculate the wafer durability rating.

Sample number	Mass classes of cubes % original mass in each class					Size-Distribution Index	Durabilty Rating (%)
	50-40gm	40-30gm	30-20gm	20-10gm	10-0gm		
1	92	---	---	---	8	368	92
2	40	48	---	---	12	304	88
3	8	47	15	10	20	213	80
4	---	40	20	18	22	178	78

Source: ASAE Standards, 1995, p. 444
Note: Example assumes original average weight/wafer is 50 gm

Results and Discussion

Wafer Stability

Post-compression Behavior of Wafers

Data showed that in all cases and for both materials, there was a uniform pattern of post-compression expansion of wafers with time in both the axial and lateral or transverse (diametral) directions. In either direction, the material expansion rate started rapidly in the first 30 to 60 minutes after formation and then slowed down to approach steady state within the observation period of 24 hours. Data indicated that a range of at least 55% up to about 100% of the total expansion took place within the

first 30 to 60 minutes. A typical case from this study is shown in Fig. (5-2) where the relative expansion was expressed as the percent of wafer expansion at a given time of wafer immediate dimension. All other wafers exhibited similar behavior.

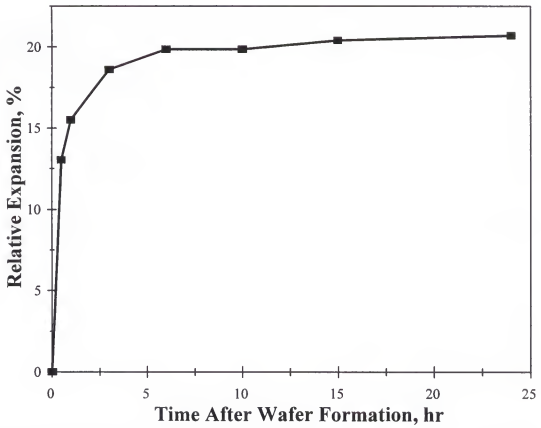

Fig. 5-2. Typical behavior of wafer post-compression expansion in the axial direction.

Similar results were reported by several researchers who worked with different biomass materials such as rice hulls, straw, grass and hay. Khankari et al., (1989), reported that rice hull wafers expanded and their density, which was directly

proportional to axial strain, decreased to a stable value (final density) within 24 hours of formation. Pickard et al. (1961) and Butler and McColly (1959) studied hay wafers and indicated that most of the wafer expansion took place in the first 30 minutes.

These findings implied that the creep recovery process almost ceased within the first 30 to 60 min. and further confirmed the viscoelastic nature of these materials as compared to an ideal elastic or viscous material (Sah et al., 1980). Additionally, it may be argued that the early rapid expansion and the following slow phase were due, respectively, to a fast elastic recovery as well as a high rate of stress relaxation followed by a continuation of the stress relaxation (dissipation) process but at a slower rate. The latter was complete within the observation period of time leaving only minimal residual stresses in the material and thus negligible expansion (O'Dogherty and Wheeler, 1984; Mohsenin and Zaske, 1976; Shepperson and Grundey, 1962).

Data also indicated that the maximum total expansion in the transverse (diametral) direction after wafers were ejected from the die was in the range of 1 to 3% of the initial transverse dimension of wafers for both materials. It was thought that this extent of expansion did not have any practical or economical importance and, therefore, was neglected. However, it provided a satisfactory justification to the assumption made in all density calculations that the wafer diameter (cross-sectional area) was equal to the internal diameter (cross-sectional area) of the die in which the wafer was made. This result agreed with results reported by other workers in the field that only minor wafer expansion took place in the diametral direction and the major expansion occurred in the direction of load application; the axial direction in this case (Mohsenin and Zaske,

1976; Huang and Yoerger, 1961; Bruhn et al., 1959). Hence, the following discussions apply to the material expansion in the axial direction only.

Wafer Final Density

In addition to being a fundamental characteristic in appraising the densification of biomass materials, wafer final density, as will be seen in the next section, is the single most important factor in determining wafer quality as expressed in terms of wafer durability. The compaction process involved compressing an amount of material (charge) of known moisture under given wafering conditions, removing it from the die at an immediate density, ρ_m, and allowing it to expand freely for 24 hours to a final density, ρ_f.

Based on this sequence of material compaction and related previous work, it was only logical to assume that wafer final density was a function of wafering conditions (P_{max}, D_c, t_h), wafer weight (charge), wafer geometry represented by its diameter and height, material moisture at the time of compaction, its immediate density, and the extent of wafer post-formation axial expansion. All these variables have a bearing on the wafer density and quality as was outlined in the review of literature. This verbal statement of the relationship between ρ_f and those variables may be transformed into a mathematical functional relationship of the following form

$$\rho_f = f(\rho_m, t_h, P_{max}, D_c, X_{max}, MC, W, H) \qquad (5\text{-}1)$$

where ρ_m is the wafer immediate density (Kg/m^3)

P_{max} is the maximum stress applied (N/m^2)

D_c is the die (wafer) diameter (m)

t_h is the hold time (sec)

H is the wafer immediate length (thickness) (m)

W is the wafer weight (N)

MC is the material moisture when compacted (%w.b.)

X_{max} is the wafer maximum relative expansion in the axial direction, fraction The term X_{max} merits a word of clarification. It was believed that in order to make fair comparisons and draw valid conclusions, X_{max} should be used in a relative rather than absolute sense. This was because wafers made even under the same conditions expanded in different proportions. Therefore, the term X_{max} was defined as the ratio of maximum (total) absolute expansion of a wafer (after 24 hours) to the initial axial dimension at zero time, i.e., it was expressed as proportion of the immediate wafer length, H.

It was convenient to divide the variables above that affect final density into two groups. The first was the wafering conditions, which included P_{max}, D_c, and t_h and the second group was called "the other variables," which included ρ_m, X_{max}, MC, W, and H. Each of these groups will be considered in turn.

Influence of Wafering Factors on ρ_f

Maximum pressure (stress). Higher P_{max} resulted in wafers with higher final density at all hold times. It was found that in the 40- and 50-mm chambers, a 40 to more than 50% increase in final density was achieved when the Pmax level was raised from 17 to 37 MPa. However, the rate of increase in final density decreased with

higher Pmax level. For instance, in the 40-mm die, ρ_f increased by only less than 9% when P_{max} increased from 37 to 58 MPa (Fig. 5-3). Therefore, in the 40- and 50-mm

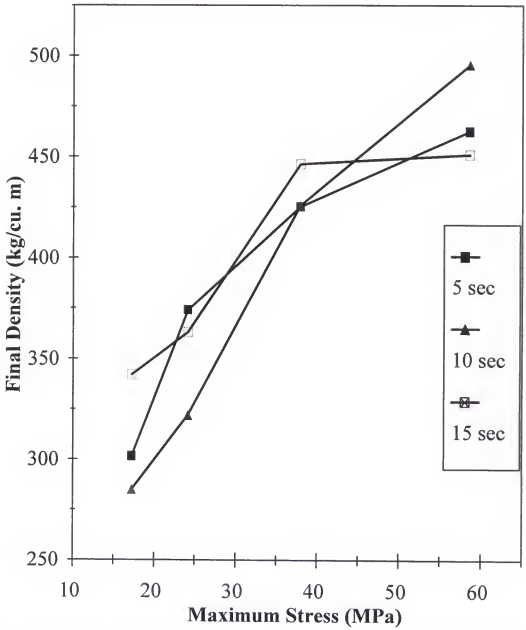

Fig. 5-3. Influence of maximum stress on wafer immediate density of elephantgrass with hold time as a parameter.

dies, applying a stress level higher than 37 MPa may not be recommended. This result is compatible with those reported by O'Dogherty and Wheeler (1984) who worked on straw and found that pressure increased exponentially with increasing final density.

As for energycane, the material response to P_{max} level in the 40-mm chamber was identical to that of elephantgrass, i.e, higher P_{max} resulted in higher ρ_f. In other chambers, the influence of stress level on final density generally showed a similar trend as that of elephantgrass although the influence of P_{max} on ρ_f in these larger dies (lower stress levels) was less evident. An attempt to explain this difference is found in the last section of this chapter.

In this type of compression, the role of P_{max} may better be appreciated by realizing that thermal effects, a major contributor to wafer bonding, were absent. In all tests conducted in this work, the temperature of the die or product did not exceed the ambient temperature. This indicated that the amount of heat produced, if any, was very small and could be dissipated instantly. For this reason, pressure was the only factor that effected mechanical and chemical bonding of the material by reorientation, flattening and crushing of material particles. Additionally, increasing P_{max} may have reduced the material resistance to compression by forcing decreases in material bulk modulus (Faborode and O'Callaghan, 1986). Higher pressures caused more of these effects leading eventually to a more stable product.

Chamber size. At any given P_{max}, the 40- and 50-mm dies produced more stable elephantgrass wafers than the larger ones at all hold times. For example, at the lowest stress (17 MPa), which was common to all dies, and a hold time of 5 sec, the final

density of elephantgrass wafers in the two smaller dies was more than 300 kg/m^3 compared to 260 kg/m^3 in the larger ones. It was reported that wafers made in smaller dies retained higher final density due to the greater mechanical bonding (interlocking) of material particles in smaller dies (O'Dougherty and Wheeler, 1984; Bruhn, 1955).

As for energycane, the effect of die diameter was not as consistent. Nonetheless, it may be stated that for both materials, it appeared that smaller wafers suffered more relative expansion than larger ones. However, due to their normally higher immediate density, they generally retained higher absolute values of final density. This matter will be considered in a more general sense in the following sections.

Hold time. Although it appeared in some cases that longer hold time was useful, Figure (5-3) showed that in both materials, different levels of t_h generally did not have a consistent effect on wafer stability represented by the final density. Rather, it depended on the levels of Pmax and Dc used. This suggested that these variables were interrelated. In statistical terms, it was believed that a significant interaction existed among these variables. To test this hypothesis, an analysis of variance (ANOVA) procedure was applied to the data using the statistical software package SAS®.

The results showed highly significant interactions at the 0.05 level among the three variables. The most important finding was a highly significant three-factor interaction (t_h*P_{max} *D_c) as may be predicted from Fig. (5-3) (Ott, 1988). This outcome mandated the statistical approach of fixing two variables (P_{max} and D_c) and looking at the third, which is t_h in this case. The results of such a test are shown in Table (5-3) for both materials. The convention was that times with a common character were not

significantly different as to their effect on ρ_f. Additionally, the times that gave best results (highest ρ_f) were put in boldface and underlined whether they were statistically different or otherwise.

The results in Table (5-3) show that the 15-sec hold time was significantly different and gave better results in only two of the 10 elephantgrass treatments. Of the seven energycane treatments, the 15-sec was different and better in three treatments. Qualitatively, it can be seen from the results (Table 5-3) that, for both materials, a 5-sec hold time was in many cases not significantly different from longer times. This appeared to indicate that in general once the material had been held under P_{max} for 5 sec, only modest improvement in the wafer final density was realized by a longer hold time. It may, then, be concluded that a 5-sec hold time is an optimum value for the compression of elephantgrass and energycane. Furthermore, it is useful to attempt utilizing hold times shorter than 5 sec in the pursuit of a more efficient compaction process.

Influence of The Other Variables on ρ_f

Inspecting the data of the two materials indicated that it was rather difficult to study the influence of each of these factors on wafer final density individually. Thus, it was seen best to conduct a multiple regression analysis procedure to produce a prediction equation incorporating all variables shown in Eqn. (5-1). Considering elephantgrass, a first-order linear multiple-regression analysis on those individual variables indicated that they accounted for more than 96% of the variation in the dependent variable.

Table (5-3). Statistical test of the influence of the different levels of hold time on wafer final density

		Material					
		Elephantgrass			Energycane		
Dc	P_{max}	Hold time[a] (sec)					
(mm)	(MPa)	5	10	15	5	10	15
40.0	58.0	AB	**A**	B	a	a	N.A.
	37.0	A	A	**A**	**a**	b	N.A.
	24.0	**A**	B	A	a	a	**a**
	17.0	A	A	**B**	N.A.	N.A.	N.A.
50.0	37.0	A	**A**	B	a	**a**	a
	24.0	A	**B**	C	a	b	**b**
	17.0	A	B	**A**	a	**b**	b
63.0	24.0	**A**	B	B	a	a	**b**
	17.0	A	A	**A**	a	a	**a**
76.0	17.0	A	A	**B**	ab	a	**b**

Note: Uppercase characters are used for elephantgrass and lowercase for energycane
Note: N.A. indicates that data is not available
[a] Times with a common character are not significantly different

It was desirable to develop a more compact prediction equation by reducing the number of independent variables. To do so, the dimensional analysis technique using Buckingham pi theorem was applied to the variables in Eqn. (5-1) and resulted in reducing it from nine variables to six π terms (dimensionless-variable groups). Due to

the absence of thermal effects, the basic dimensions were limited to mass (M), length (L), and time (T) and the three repeated variables chosen were W, D_c, and ρ_m.

The analysis showed that the wafer final density (Eqn. 5-1) may be described by the dependent π term

$$\pi_1 = \frac{\rho_f}{\rho_m}$$

$$\pi_2 = X_{\max}$$

$$\pi_3 = MC$$

$$\pi_4 = \frac{H}{D_c}$$

$$\pi_5 = \frac{P_{\max} D_c^{\,2}}{W}$$

and

$$\pi_6 = \frac{t_h \sqrt{W}}{D_c^{\,2} \sqrt{W}}$$

Therefore, the functional relationship for this problem may be expressed as

$$\pi_1 = f(\pi_2, \pi_3, \pi_4, \pi_5, \pi_6)$$

or,

$$\frac{\rho_f}{\rho_m} = f(X_{max}, MC, \frac{H}{D_c}, \frac{P_{max} D_c^2}{W}, \frac{t_h \sqrt{W}}{D_c^2 \sqrt{\rho_m}}) \quad (5\text{-}2)$$

A first-order linear multiple-regression model of the following form was applied

$$\pi_1 = \beta_0 + \beta_1 \pi_2 + \beta_2 \pi_3 + \beta_3 \pi_4 + \beta_4 \pi_5 + \beta_5 \pi_6 + \varepsilon \quad (5\text{-}3)$$

where ε is an error term.

It was found that all the pi terms as well as the estimated parameters had a significant effect on ρ_f/ρ_m at the 0.05 level with a coefficient of determination (R_d^2) of about 0.865 (R_d = 0.93) as shown in Table (5-4). The regression analysis, which estimated the parameters β_i, provided the following prediction equation

$$\frac{\rho_f}{\rho_m} = 0.9441 - 0.0051\pi_2 - 0.0035\pi_3 + 0.0787\pi_4 + 4.72e-8\pi_5 - 2.811e-4\pi_6 \quad (5\text{-}4)$$

or,

$$\rho_f = \rho_m (944.1 - 5.1\pi_2 - 3.5\pi_3 + 78.7\pi_4 + 4.72e-5\pi_5 - .2811\pi_6) 10^{-3} \quad (5\text{-}5)$$

Notice that higher X_{max}, MC and $\frac{t_h \sqrt{W}}{D_c^2 \sqrt{\rho_m}}$ give lower final density but an increase in ρ_m and the other two terms, namely, $\frac{H}{D_c}$ and $\frac{P_{max} D_c^2}{W}$ increases density.

Table (5-4). The SAS output of regression analysis of final density of elephantgrass .

Source	DF[a]	SS[b]	MS[c]	F[d] value
Model	5	1.1603	0.23206	376.9
Error	294	0.1810	0.00062	
Total	299	1.3413		

Variable	Parameter estimate	Standard error	t value	Prob > |T|[e]
Intercept	0.9441	0.01864	50.66	0.0001
π_2	-0.0051	0.00013	-40.40	0.0001
π_3	-0.0035	0.00123	- 2.81	0.0054
π_4	0.7873	0.02368	3.33	0.0010
π_5	4.72E-8	1.0E-08	4.73	0.0001
π_6	-2.81E-4	4.85E-5	- 5.80	0.0001

[a] DF stands for degrees of freedom
[b] SS stands for sum of squares
[c] MS stands for mean sum of squares
[d] F is the value of the F-statistic
[e] A value of less than 0.05 means the parameter is significant

It is clear that larger expansion causes proportional increase in wafer volume, which results in lower density. Material moisture, MC, plays a dominant role in the densification of biomass. Although it is believed that wafers were produced within the "optimum" moisture range, it appears that most of the work was done in the upper portion of that range. Thus, the higher or extra moisture was trapped in the material

cells resisting applied pressure and preventing close contact between material particles. Thus the higher moisture prevented the destruction of material cells and the release of the natural binding materials.

In addition, higher moisture increased the product elastic response (spring back) upon unloading especially the stem portion of material (Rehkugler and Buchele, 1967; Pickard et al., 1961). O'Dogherty and Wheeler (1984) studied the influence of MC in the range of 10 to 30% on the final density of straw wafer and reported an exponential decrease in ρ_f with increasing MC. A similar result was reported by several other workers (Bruhn et al., 1959).

It was difficult to attach physical significance to the term $\frac{t_h\sqrt{W}}{D_c^2\sqrt{\rho_m}}$. However, it may be said that it represents the net result of the interactions and trade-off effects between all the variables included in the term.

The immediate density of a wafer has a pronounced effect on the density the wafer retains after relaxation. Everything else being equal, wafers with larger ρ_m will retain higher final density. It was found that wafers with higher ρ_m maintained higher ρ_f even when they suffered significantly higher expansion than those with lower ρ_m.

The term $\frac{H}{D_c}$ represents the wafer geometry. In particular, it expresses the relative thickness of wafers, where higher $\frac{H}{D_c}$ value indicates a thicker wafer. The favorable effect of this term on ρ_f may be explained by arguing that wafer fibers at the ends are interlocked from one side only and thus are weaker and more vulnerable to expansion and even disintegration than other internal fibers. Since the portion (fraction) of fibers at the ends is higher in thin than in thick wafers, those with larger $\frac{H}{D_c}$

retained higher ρf (Butler and McColly, 1959). The term $\frac{P_{max} D_c^2}{W}$ was described by Rehkugler and Buchele (1969) as representing the stress applied on the material. It was made clear earlier that higher stress resulted in denser and more stable wafers.

A comparison between the final density values predicted by the model (Eqn. 5-3) and measured values of ρ_f from experimental data is shown in Fig. (5-4). The correlation coefficient, R_c^2, of measured with predicted values of ρ_f was about 0.97; a perfect correlation would have an R_c^2 value of unity. It is noted that a few points were outliers in the measured final density range of 300 to 400 kg/m^3. The model has overestimated these values in this range. However, only eight of the three-hundred points were as such, which is not expected to have any significant effect on the suitability of the model in predicting the final density of elephantgrass wafers.

The same approach was carried out on the data of energycane. It was found that all variables, except material moisture, were highly significant at the 0.05 level of significance (see Appendix E). It was also found that almost 96% of the variation in ρ_f was attributed to those individual variables. Unfortunately, however, it turned out that a regression model on the same non-dimensional groups (π terms) developed for elephantgrass gave poor results. This was likely due to the highly significant interactions that existed among several variables including the repeated variables, which appeared in more than one dimensionless group. In other words, the variables might have been so interrelated that they masked (canceled) one another's effect. Therefore, the final density of energycane wafers was correlated to those individual variables by a multiple regression equation.

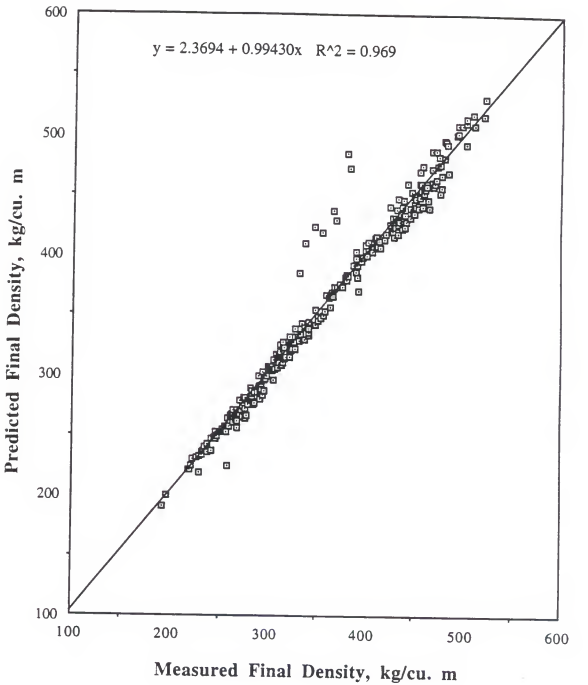

Fig. 5-4. Predicted versus measured values of elephantgrass final density.

It was intended to develop a simple prediction equation without significantly sacrificing the model accuracy. It was found that including interaction terms resulted in a cumbersome and lengthy equation without substantially improving the coefficient of determination, R_d^2. Thus, the best suggested model was of the following form

$$\rho_f=\beta_0+\beta_1 t_h+\beta_2 P_{max}+\beta_3 D_c+\beta_4 X_{max}+\beta_5 \rho_m+\beta_6 W+\beta_7 H+\beta_8 MC+e \qquad (5\text{-}6)$$

where e is an error term. Substituting the values of β_i from the SAS output gives

$$\rho_f=-1417.97+1.65t_h+(1.36E-6)P_{max}+22428.23D_c-1.43X_{max}+1.72\rho_m-40.40W+29351.82H-2.26MC \qquad (5\text{-}7)$$

All parameters were found highly significant at the 0.05 level except that attached to material moisture, MC, which is consistent with the significance of the variables themselves. A detailed description of the SAS output is found in Appendix E. Though, it was decided to keep that important term based on the statistical interpretation that an insignificant parameter did not mean the factor did not influence the dependent variable, rather, it meant that the influence of that variable is small compared to other variables (Ott, 1988). It may be added that the extent of variation of MC was within a small range so that it did not have a highly significant effect on ρ_f.

It is readily noticeable that a longer t_h, higher P_{max}, and larger ρ_m, D_c and H result in a product with higher final density while larger values of X_{max} and W lead to wafers with lower ρ_f. The roles of P_{max}, ρ_m, and X_{max} were discussed above for the case of elephantgrass and are still applicable for energycane. It was indicated previously that

the longer hold time appeared to contribute to producing wafers with higher ρ_t. Longer t_h may give material particles a time window to reorient and interlock and allow the creep deformation of the material to proceed and stabilize under the maximum load. Such a result was indicated by others working in the compression of biomass materials (Bruhn, 1955; Bruhn et al., 1959; Reece, 1965). For a given diameter, higher values of H meant thicker wafers. The favorable effect of thicker product on the final density was addressed above.

The model also indicates that energycane wafers with larger diameters were more stable. A possible explanation may lie in arguing that larger energycane wafers had a larger number of interlocking fibers. Moreover, it appears that since larger wafers were thinner (smaller $\frac{H}{D_c}$) than smaller ones, better pressure transmission through the material resulted in better stress distribution in the material. It is likely that these two effects more than offset the advantages of higher quality particle interlocking and lower fraction of weak particles at the wafer surfaces present in smaller dies. Therefore, wafers with smaller diameter suffered more expansion relative to their immediate dimensions and in general retained smaller fraction of their immediate density.

As for the material weight, W, it seems that larger charges of energycane caused more friction among the material fibers and between the material and die walls. This resulted in absorbing substantial amounts of the compression energy (Butler and McColly, 1959). An additional possible effect of larger W may be poor pressure transmission through the material resulting in poor stress distribution in the wafer

(Faborode and O'Callaghan, 1986; Rehkugler and Buchele, 1969). Those effects combined to produce a wafer of lower final density. The values of ρ_f predicted by this model versus the measured values of ρ_f for energycane are shown in Fig. (5-5) with a correlation coefficient (R_c^2) of 0.956. It can be seen from the figure that the model has relatively overestimated some values of final density and underestimated others in the range below 300 kg/m^3. In the upper range, the model provided much better estimates. This is a positive outcome because the higher range was considered the useful range because it generally corresponded to wafers of good quality.

It may be concluded in this regard that these models were adequate in describing wafer final density as was demonstrated by the coefficients of determination, R_d^2, correlation coefficients, R_c^2, and levels of parameter significance. Nevertheless, other factors that were believed to be important were omitted from this analysis including the biomechanical and biochemical properties of these materials such as the material moduli and amounts of natural bindings (pectin and lignin) in their tissues. In addition, an accurate evaluation of material composition in terms of the stem/leaf proportions and their characteristics may add more information to the study of wafer quality.

Wafer Durability

Preliminary examination of the data showed that durability, under a given set of wafering parameters, was determined primarily by wafer stability, which was characterized by final density. The higher the final density, the better the durability

(Khankari et al., 1989; O'Dougherty and Wheeler, 1984; Balk, 1964). To quote from Mohsenin and Zaske (1976) "It is a well established fact that higher density wafers

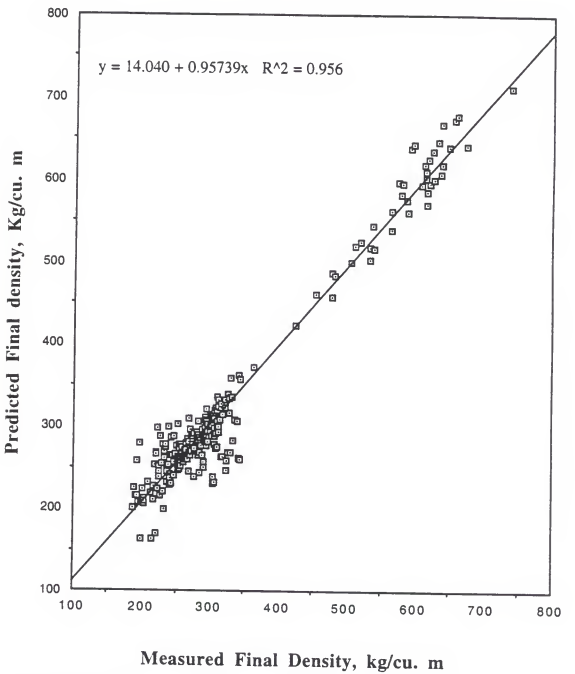

Fig. 5-5. Predicted versus measured values of energycane final density.

result in more stable and durable wafers". It is evident that this sequence of dependency is compatible with the sequence of material compaction as presented earlier.

The initial test of results also revealed another important conclusion. It is believed that the press capacity (10 tons) was sufficient for small scale practical compaction applications. Nonetheless, the highest P_{max} achieved at the press maximum capacity in the 63- and 76-mm chambers was 24 and 17 MPa, respectively (Table 3-1). The press failed to produce durable wafers in all runs for both materials in these dies, that is, wafer durability in these chambers was always below 70%. Moreover, it was not possible to assess the performance of these dies at higher stresses due to lack of data. Accordingly, the following discussions will focus on wafer durability in the 40- and 50-mm chambers. The use of available data from the larger compression cylinders will be limited to comparison purposes with the smaller dies whenever appropriate.

Durability vs. Wafer Final Density

Data showed that, under any given set of wafering conditions, more stable wafers, i.e., wafers with higher final density, were consistently more durable. This result applied with some exceptions to all four dies for both materials. This led directly to the conclusion that wafers made in the smaller dies under higher stresses were the most durable simply because they were the most stable. These findings amplify the role of final density and, consequently, P_{max} and chamber size in the production of wafers of acceptable quality as outlined earlier.

For a given size, final density is the density of wafers prior to tumbling. It should be clear that wafers with higher ρ_f generally retained stronger-bonded particles

and could generally withstand the impacts and shearing during tumbling. Therefore, they suffered less weight loss and possessed better durability. Table (5-5) shows the data relating final density to durability in the two smaller dies.

Table (5-5). The role of wafer final density in the determination of wafer durability.

			Material			
			Elephantgrass		Energycane	
D_c (mm)	P_{max} (MPa)	t_h (sec)	ρ_f	D.R.[a]	ρ_f	D.R.
40.0	58.0	5	441.2	81.5	617.1	97.5
		10	495.7	87.6	627.9	97.0
		15	462.8	83.7	N.A.	N.A.
	37.0	5	446.5	72.8	593.0	97.1
		10	426.0	83.3	492.0	96.8
		15	425.4	91.2	N.A.	N.A.
	24.0	5	363.1	90.4	283.3	81.6
		10	322.2	80.5	272.3	78.1
		15	374.1	88.0	292.1	75.0
	17.0	5	442.3	85.0	N.A.	N.A.
		10	285.1	82.1	N.A.	N.A.
		15	301.8	91.8	N.A.	N.A.
50.0	37.0	5	445.8	89.6	291.4	77.0
		10	450.3	91.2	305.6	79.9
		15	409.1	88.9	285.0	61.8
	24.0	5	403.9	83.4	304.8	34.2
		10	433.8	88.2	290.9	78.2
		15	328.4	77.6	200.8	73.6
	17.0	5	313.9	63.5	281.9	26.0
		10	289.4	69.7	305.9	73.7
		15	328.1	78.0	225.7	74.6

[a] D.R. stands for durability rating (%)

Note: N.A. means data is not available

The minimum final density required for durable wafers for both materials ranged from 290 to 320 Kg/m^3 depending on chamber size. This was equivalent to an immediate density of roughly 400 to 420 Kg/m^3 to account for wafer expansion. In the two smaller dies, 17 to 24 MPa was sufficient to produce this range of final density. Including all dies, the final density was, on the average, approximately 75% of the immediate density for elephantgrass and 72% for energycane.

Analysis of Forces During Tumbling

In addition to the wafer final density and the related factors, the forces imposed on wafers during tumbling are believed to be an important factor in effecting the difference in durability rating between the smaller compression cylinders (40- and 50-mm) and larger ones. A simplified analysis of forces the wafers are subjected to in the tumbler was conducted in an attempt to shed more light on the causes of durability differences among those dies.

The analysis was hinted by the finding that wafers with a given final density made in the smaller dies were more durable than those made in larger ones with the same or even higher final density. A good example is the finding that larger energycane wafers, as mentioned earlier, had generally higher ρf but still were less durable. It was clear that ρf alone failed to provide a reasonable explanation for such cases.

It was pointed out before that the major forces involved during wafer handling were impact and shearing. If wafer impact on the tumbler walls during tumbling is simulated as a free fall, which is a conservative assumption, it is clear that the kinetic

energy the wafers must absorb upon impact is directly proportional to the wafer terminal velocity, that is,

$$K.E. = \frac{WV^2}{2g} \tag{5-8}$$

where K.E. is the wafer kinetic energy

W is the wafer weight

V is the wafer terminal velocity

g is the acceleration due to gravity

Since the fall occurs in a conservative force field (gravity), the principle of conservation of mechanical energy may be applied. Thus, it may be stated that

$$\frac{WV^2}{2g} = Wh$$

where Wh is the product of wafer weight and fall height (potential energy)

h is the average fall height

From Eqn. (5-6), the velocity is given by

$$V = \sqrt{2gh} \tag{5-9}$$

substituting the expression for V into Eqn. (5-5) gives

$$K.E. = Wh \tag{5-10}$$

The last equation states that the severity of impact varies directly with wafer weight and average height of wafer fall, h. The latter was assumed constant for all wafers since

they were all tested in the same tumbler. Therefore, the impact severity is determined solely by wafer weight.

Shearing forces, F_s, are caused by friction effects due to the rubbing of wafers against each other and/or against tumbler walls. If shearing stress, τ, resulting from friction is assumed constant for all wafers, which is a reasonable assumption based on using the same material and same tumbler, the resulting total shearing force is given by

$$F_s = \tau A_s \tag{5-11}$$

where A_s is the surface area of the wafer.

Eqn. (5-8) shows the shearing force exerted on a wafer is proportional to its surface area.

Based on the analysis above, heavier wafers and wafers with larger surface areas, both of which apply to wafers made in larger dies, experience more severe impacts and, thus, are exposed to more shattering of their particles both on the surface and along weak planes within wafers. It is speculated that such weak planes may well exist due to filling each charge in the die on several strokes. Further, larger wafers are subject to larger shear forces, which impose a more serious abrasive action on wafer surfaces and edges, which are the weakest and most vulnerable parts of wafers as explained earlier.

The sum of these actions contribute to wafer weight loss during tumbling due to production of fines and wafer partial disintegration, which lead to wafers of lower durability rating. To relate this analysis to this study, it may be pointed out that the

weight and surface area of a 76-mm wafer were, respectively, about 2.2 and 2.8 times that of a 40-mm wafer (see Table 3-2). Accordingly, it may be concluded that larger impact and shearing forces on larger wafers play an important role and, in part, explain the advantage of smaller dies in comparison to larger ones in producing wafers of better durability ratings.

It is noteworthy that in addition to the two major determinants of durability discussed above, namely, final density and impact and shear forces, there are other considerations that may have a significant effect on wafer durability. The product moisture at the time of tumbling comes into play as one major factor. In particular, if wafers loose significant amounts of moisture between the time of formation and testing, they become vulnerable to disintegration when tumbled. The reason for this is the critical role of moisture in the binding of material particles as mentioned elsewhere in this text.

In fact, the ASAE standard procedure for durability test of wafers requires specifying the time period elapsed between wafer formation and tumbling and the wafer MC when tumbled. Table (5-6) shows the product MC at the time of tumbling for the two smaller dies.

Comparison of the two Materials

The quality of elephantgrass and energycane wafers was compared in the two smaller dies. Data showed that elephantgrass wafers were superior to energycane wafers in all cases except in the 40-mm die at the 37 and 58 MPa. Energycane wafers

Table (5-6). Moisture content in % (w.b) of wafers made in the 40- and 50-mm dies at the time of tumbling.

D_c (mm)	P_{max} (MPa)	t_h (sec)	Wafer Moisture % Elephantgrass	Energycane
40.0	58.0	5	16.5	13.8
		10	12.8	14.5
		15	16.0	---
	37.0	5	15.7	15.9
		10	17.5	16.6
		15	17.6	---
	24.0	5	17.9	15.4
		10	19.2	16.8
		15	18.5	14.0
	17.0	5	18.5	14.2
		10	---	17.0
		15	13.3	19.9
50.0	37.0	5	14.8	14.5
		10	15.0	14.3
		15	15.5	17.5
	24.0	5	15.3	13.8
		10	14.4	14.5
		15	14.0	---
	17.0	5	11.4	16.3
		10	14.6	14.2
		15	10.1	14.5

Note: all wafers were tested 24 hours after formation

under those conditions were significantly higher in immediate density, experienced much less expansion, and, therefore, possessed higher final density and durability (see Table 5-5). In contrast, the rest of energycane wafers expanded excessively and

possessed poorer quality. It was found that, under lower stresses ($P_{max} < 37$ MPa), energycane wafers expanded 65% more than elephantgrass wafers. Under higher stresses ($P_{max} > 37$ MPa in the 40-mm die), the expansion experienced by energycane wafers was only 50% of that of elephantgrass wafers. These figures refer to the maximum expansion, X_{max}, as defined earlier.

In this study, the two materials were investigated in terms of their relevant differences in this regard in only two aspects. The first was the crude protein content (CP), which was performed in the Forage Evaluation Support Laboratory of the Agronomy Department at the University of Florida. The second was the stem/leaf proportion which was assessed by observation. These aspects may help provide a partial explanation of the difference in wafer quality between the two materials.

Energycane variety used in this work was significantly higher in stem content than elephantgrass. The latter was characterized as leafy compared to the former. Several studies addressed the influence of this factor on biomass compaction. It was generally agreed that stems, as compared to leaves, were more resilient, possessed stronger mechanical structure and were low in protein content (Mohsenin and Zaske, 1976; Rehkugler and Buchele, 1967). For these materials, though, the analysis showed that the CP content of energycane was on the average about 8% more than that of elephantgrass.

It appeared that energycane wafers under low P_{max} levels stored large amounts of energy during compression due to the high resiliency of the high stem portion of the material. That energy was later released during product relaxation. On the other hand,

the strong stem structure clearly required higher loads to enforce effective flattening and crushing of material particles on one hand and to release the natural bonding agents on the other. Failure to produce either effect resulted in the excessive expansion and low final density and durability of energycane wafers. In contrast, it seemed that only the highest pressure levels applied in the 40-mm die induced permanent particle bending and sufficient destruction of cell structure of energycane particles to cause permanent (plastic) bending and the release of bonding components (protein). The higher protein content of energycane resulted in wafers of superior quality under these conditions.

As for elephantgrass, the less resilient and fragile structure of the large leaf proportion made it easier for high as well as lower stress levels to make wafers of good durability. Therefore, compared to energycane, essentially all stress levels induced permanent bending and better interlocking of material particles, which resulted in less wafer expansion upon unloading. In addition, applied stresses caused effective destruction of the material structure and, thus, freed the natural binding materials, which resulted in a more stable product.

It should be emphasized, however, that energycane wafers were of better quality only in a few limited cases. In the vast majority of cases, elephantgrass wafers were favorable in quality to those made of energycane as indicated above.

CHAPTER 6
COMBUSTION CHARACTERISTICS OF WAFERS

Introduction

The previous two chapters covered the first quality aspect of wafers regarding their formation characteristics and quality. Since wafers are intended to be used as fuel, this chapter shall cover their second quality aspect where the combustion of wafers in a small stove is studied. Phases of combustion, time history of temperature inside and outside the stove, stove performance, effectiveness of the brick insulation, exhaust gas composition and influence of compaction (wafering) conditions on wafer combustion are considered.

In evaluating the potential of a material as fuel, a few basic tests such as energy and chemical analyses are necessary. The purpose of energy analysis is to determine the heating value (HV), also known as calorific value, of the material. The HV is a measure of the amount of energy contained in a unit mass of material. The chemical analysis, including proximate and ultimate analyses, is aimed at revealing the material composition relevant to combustion. An additional useful and necessary analysis, which

may be considered part of the chemical analysis, is the ash analysis. Its purpose is to determine the major mineral (inorganic) elements contained in the material tissues.

Based on these analyses, the material potential as an acceptable source of energy in terms of combustion air requirement for satisfactory burning, material potential of air pollution and health hazard and possible slagging or fouling problems upon burning are evaluated. The energy analysis (HV) and chemical analysis (proximate and ultimate) of selected samples of elephantgrass and energycane reported by the commercial laboratory are shown in Table (6-1).

Review of Literature

As in coal, the major solid fossil fuel, carbon is the primary source of energy in biomass fuels and accounts for most of the energy released when burning the fuel. Combustion of biomass takes place by the oxidation of carbon and hydrogen, both of which are exothermic reactions. The combustion process proceeds in three consecutive but overlapping stages. Initially, material moisture must be driven off in an endothermic isothermal process. Next, pyrolysis results in volatilization and oxidation of volatiles, which initiates an intensive flaming combustion. Finally, carbon left after volatiles have been released is oxidized effecting a slower glowing combustion (Elliott, 1980; Shafizadeh, 1981).

Table (6-1). Energy and chemical analyses of elephantgrass and energycane

Analysis	Elephantgrass		Energycane	
	As Received	Dry	As Received	Dry
Proximate				
Moisture	8.64	0.00	10.68	0.00
Ash	2.40	2.63	3.87	4.34
Volatiles	73.73	80.70	72.11	80.73
Fixed Carbon	15.23	16.67	13.34	14.93
Total	100.00	100.00	100.00	100.00
Ultimate				
Moisture	8.64	0.00	10.68	0.00
Carbon	45.65	49.96	43.40	48.59
Hydrogen	5.22	5.72	5.06	5.67
Nitrogen	0.29	0.32	0.32	0.36
Sulfur	0.08	0.09	0.08	0.09
Ash	2.40	2.63	3.87	4.34
Oxygen	37.72	41.28	36.59	40.95
Total	100.00	100.00	100.00	100.00
HHV (kJ/kg)	17235	18865	16350	18300

It is anticipated that grass wafers will burn as well as wood pellets if brought to the proper MC and density (Erikson and Prior, 1990). This may be based on the fact that these grass materials should burn as well as wood (Beck and Halligan, 1980). Green et al. (1991) successfully blended and burned biomass materials, including loose elephantgrass and energycane, with non-hazardous waste materials and natural gas.

When considering biomass as fuel, the following characteristics are considered critical: physical properties including MC, bulk density and particle size; and chemical properties including heating value, ash content and composition. Other cost-related factors such as market, availability, and transportation, which are highly site specific, should also be considered (Beck and Halligan, 1980; Miles et al., 1993). Moisture content (MC) for biomass fuels should not exceed 30% to 40% for direct combustion and if storage is a factor should be less than 15% to 20%.

The ash value of biomass materials in general is considered relatively high and poses a problem upon burning. High ash content lowers the so-called ash fusion temperature (also known as softening, sticky or melting temperature) to typically 700 to 760 C (1350 F) as compared to 1300 C (2400 F) for wood fuels. This eventually leads to ash build-up (fouling) or what is known as the slagging problem in furnaces (Miles, 1995 and 1992).

The high concentrations of alkali metals, particularly potassium and sodium that exist mainly as oxides aided with the presence of silica, are the major contributors to the problem. It may be pointed out, however, that, compared to large-scale applications, the slagging problem in small-scale domestic applications is much less serious due to lower temperature, seasonal operation, small size and simple structure. Therefore, the consequences of fouling most relevant to residential applications is perhaps limited to the need for frequent cleaning (Johnston, 1995).

In attempting to predict slagging, it was recommended that, in addition to the proximate and ultimate analyses, fuel elemental composition, alkali concentration,

sulfur, and silica analyses be made because they are the best indicators. Among the means utilized to alleviate the slagging problem included using additives such as lime and clays, and mixing "premium" fuels, i.e. fuels with ash content of less than 0.5% to 1%, with high alkali fuels. These measures aimed at raising the fusion temperature above that of the furnace. On the other hand, boiler and stove manufacturers are working on the design aspects such as devising self-cleaning stoves, adding soot blowers, and more importantly attempting to design new generation of furnaces that are less fuel-sensitive and are capable of efficiently burning low grade fuels (Johnston, 1995).

As indicated earlier, biomass in its natural form, is generally an inefficient fuel due to its low bulk density and high moisture content. Therefore, densification of the materials into wafers constitutes an upgrading process. It increases the material "energy density", reduces the size of feeding and burning equipment and improves the material flowability. Moreover, it adds several advantages including a rate of combustion comparable to that of coal with less sulfur oxide and NO_x, provides uniform combustion, and alleviates the problem of particulate emissions (Balatinecz, 1983). Additionally, compared to unconsolidated material, the compact product is more attractive as a feedstock for gasification and is safer to store because the possibility of spontaneous combustion and biological deterioration is significantly reduced (O'Grady et al., 1980; Balatinecz, 1983).

Densified biomass was considered a good fuel candidate for residential heating systems as well as wood stoves (O'Grady et al., 1980). Petrie and Baldwin (1992) listed

fuel ignitability, combustion characteristics, smoke evolution, and ash residue among the most important properties of a fuel as a domestic substitute. The authors also studied the combustion of some densified wastes, some of which are of biomass origin. They indicated that the combustion proceeded in three phases, namely, ignition delay, devolatilization and char combustion and concluded that these materials have a significant potential to substitute for traditional fuels.

Reed and Bryant (1978) stated that the technology for using densified biomass as fuel was well developed, particularly for large-scale applications but added that this form of fuel had a potential for fueling residential heating systems as well as wood stoves. On the other hand, Bhattacharya et al. (1989) characterized densified biomass in general as having a poor combustion quality due to their low ignitability, slow burning and excessive smoke production. However, the authors acknowledged that there were several means to increase the combustion quality of compacted biomass fuels. Moreover, White and Plaskett (1981) indicated that although slow burning was impractical industrially, it might be acceptable in domestic applications.

The two emissions of concern when burning biomass are particulates and carbon monoxide (Braunstein et al., 1981). They result primarily from incomplete combustion of the fuel. Hence, in addition to being a health hazard, particulates and carbon monoxide emissions represent energy loss and, thus, should be minimized. Compared to the major solid fossil fuel (coal), biomass fuels tend to be much lower in sulfur and nitrogen content and achieve much lower flame temperatures when burned. Therefore,

very low, if any, emissions of sulfur oxide , SO_2, and nitrogen oxides, NO_x, two major pollutants, are encountered (Beck and Halligan, 1980).

Materials and Methods

For studying the combustion of wafers, they had to be burned and monitored. To do so, a 30 by 30 by 30 cm stove with a 15 by 15 cm front door was constructed in the shop. It was made of 6-mm thick sheet metal and lined with fire brick on all surfaces, except the floor, to provide proper insulation. A 10-mm thick sheet metal covered the floor of the stove to withstand combustion temperature. A 127-mm diameter, 90-cm high stack was fitted on the upper surface of the stove.

Along one side of the stove, several optional slots (vertical narrow rectangular openings) intended to supply natural air to the stove were made at the level of the combustion floor. They later proved to be inadequate because on the one hand, they were insufficient to establish and sustain combustion and, on the other hand, released large amounts of smoke. Therefore, they were kept closed throughout all experiments and only forced air was provided.

Forced air was supplied by a fixed-speed electric fan (Dayton Model No. 4C443A) attached to the rear corner of the stove. However, the fan provided much more excess air than was required. To overcome this problem, a movable thin metal plate was placed over the fan intake and was used to vary the fan suction area to provide the adequate rate. The initial estimation of combustion air required was based

on the ultimate analysis of materials. Table (6-2) shows the method of calculating the theoretical (stoichiometric) air necessary for complete combustion of 100 kg of elephantgrass and a mass balance of the inputs and outputs of combustion is shown in Table (6-3). The same procedure was followed for energycane and the results are reported in Table (6-4). The actual air provided was measured using a digital Omega anemometer. It was calculated that 70 and 80% excess air was supplied for elephantgrass and energycane, respectively.

Fig. 6-1. A general pictorial view of the stove used in combustion tests.

The figure above (Fig. 6-1) portrays a general view of the stove. The figure shows stove door, stack, forced-air fan in addition to some other equipment used and arrangements made during the combustion tests. Also shown in the picture are the thermocouple wires and probes used for temperature measurement.

Table (6-2). Determination of theoretical air and products of complete combustion of 100 kg elephantgrass.

Comp.	Weigh (kg/100kg)	Moles	Required (moles)		Products[a]			
			O_2	N_2	CO_2	H_2O	SO_2	N_2
C	45.65	3.8000	3.80	14.30	3.80	--	--	--
H_2	5.22	2.6100	1.31	4.91	--	2.61	--	--
O_2	37.72	1.1800	-1.18	-4.44	--	--	--	--
N_2	0.29	0.0100	--	--	--	--	--	14.79
S	0.08	0.0025	0.0025	0.0094	--	--	.0025	--
H_2O	8.64	0.4800	--	--	--	0.48	--	--
Total			3.928	14.78	3.8	3.1	.0025	14.8

Note: Air Required=3.9275*32+14.78*28=539.53 kg air/100 kg elephantgrass.
[a] The double hyphen is used to denote null.

For each material, seven different samples of wafers, each weighing 250 to 500 grams, were prepared under the selected wafering conditions shown in Table (6-5). The scheme chosen was such that comparisons between wafers made in the same die different stress levels as well as at the same stress in different dies could be made. All wafers were made at a hold time of 10 sec. Wafer samples with about 15% moisture

Table (6-3). Mass balance of complete combustion of 100 kg elephantgrass

Inputs (kg)		Outputs (kg)
Material = 100.00		CO_2 = 167.20
Air = 539.53		N_2 = 414.13
		SO_2 = 0.16
		H_2O = 55.62
		Ash = 2.40
Total	639.53 kg	639.51 kg

Table (6-4). Theoretical air and mass balance of complete combustion of 100 kg energycane.

Inputs (kg)		Outputs (kg)
Material = 100.00		CO_2 = 159.14
Air = 513.85		N_2 = 394.46
		SO_2 = 0.16
		H_2O = 56.21
		Ash = 3.87
Total	613.85 kg	613.84 kg

content (w.b.) were fed into the stove by hand and a torch was used to initiate the combustion process after turning the forced air fan on.

Table (6-5). Selected wafering conditions for combustion tests. A 10-sec hold time was used for all runs.

Diameter (mm)	Maximum stress (MPa)	
40.0	17.0	37.0
50.0	17.0	37.0
63.0	17.0	24.0
76.0	17.0	

Attempts to burn the wafers failed due to their low ignitability. Therefore, small amounts of diesel fuel were sprayed onto the wafers and effectively assisted in initiating the burning process, which proceeded successfully toward the end. A 10- to 15-minute break separated consecutive runs to allow for cooling the stove and thermoprobes, cleaning the stove, and collecting ash samples.

The manner in which the wafers burned was observed through the front door. The door was made of 17-mm thick steel. During the time the material combustion was observed, the door had to be in the open position. The major criteria monitored included combustion sustainability, burning rate and time, slagging potential, and changes experienced by the wafer physical shape and integrity.

In addition to monitoring and observing the combustion process, the experimental plan for combustion included temperature measurement and ash analysis. It was decided to measure the temperature in four stove locations. Two K-type thermoprobes were used to measure the flame temperature, T_f, and the stack temperature, T_s, which is the temperature of gases right before entering the stack. The

probes were inserted into the combustion zone through small holes made through one side of the stove.

Two T-type thermocouples were used to measure the insulation temperature, T_i, at the fire brick-metal interface in an attempt to study the insulation effectiveness of the fire brick lining in impeding heat loss from the stove. The thermocouples were placed in two locations; one on top and the other on one side of the stove. Two small grooves were made in the brick to secure the thermocouple wires in place. All thermocouples were connected to a data acquisition system set at 30 or 60 seconds per reading.

Two additional T-type thermocouples were utilized separately to measure the exhaust gas temperature at the upper end of the stack and the material temperature during compression. The purpose of the former measurement was to obtain a more realistic reading of the temperature of flue gases and the purpose of the latter was to test for thermal effects, namely, changes in material temperature while being compressed.

Representative samples of both materials were prepared and sent to the Analytical Research Laboratory at the University of Florida for ash analysis. Similar samples each weighing 300 gm were chopped and placed in safe containers and were sent to Hazen Research, Inc., Golden, Colorado where the energy (HV) and chemical analyses (ultimate and proximate) were conducted.

Results and Discussion

The Combustion Process

The combustion tests conducted showed that wafers of both materials possessed unfavorable ignition characteristics. This was demonstrated by a difficulty to start the combustion process. However, once ignited, the materials burned satisfactorily to the end. They effectively sustained combustion especially when properly exposed to and sufficiently supplied with combustion air. From observation, it was noticed that the combustion process in all cases started with an intense flame combustion that dominated this initial phase followed by an apparently less intense combustion of material particles starting at the outside surfaces.

These observations were confirmed by examining the time history of flame temperature, T_f. Data showed that burning started at the pre-combustion stove temperature followed by a rapid increase in T_f to a peak value. This was evident from the sharp slope of T_f curve versus time in the initial stage. After reaching a peak, T_f decreased in a roughly exponential fashion to a steady state value till the end of the combustion process. The variation in T_f through the combustion period is shown in Fig. (6-2) and Fig. (6-3).

The discussion presented above clearly confirms that the combustion of elephantgrass and energycane proceeded in the last two of the three generally distinct phases of biomass combustion in the correct order. The intense flame combustion

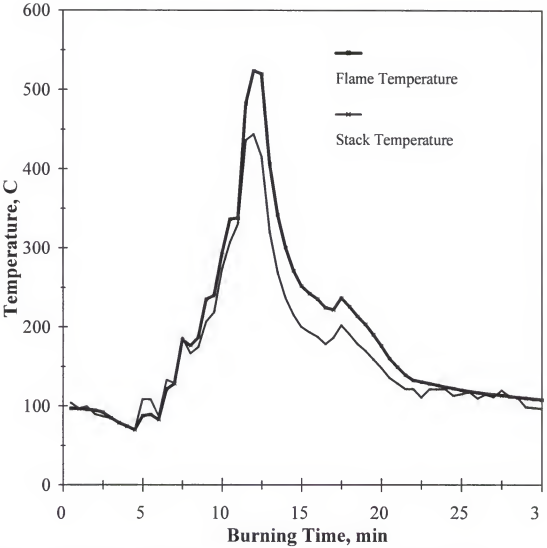

Fig. 6-2. Variation of flame and stack temperature during the combustion of elephantgrass wafers.

mentioned above corresponded to the inherently rapid evolution (volatilization) and flamy combustion of volatiles contained in the material while the combustion of material particles corresponded to the so-called char or glowing combustion, a characteristically slower process.

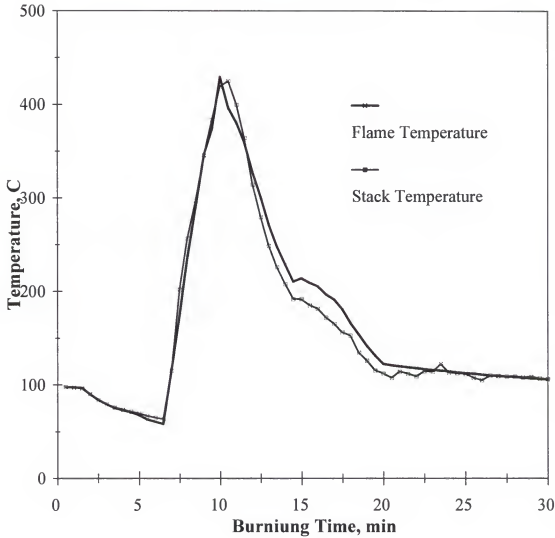

Fig. 6-3. Variation of flame and stack temperature of during the combustion of energycane wafers.

Like all biomass, the combustion of these materials must start with the first phase, which involves the isothermal evaporation of moisture. The lack of a clear indication of the first phase in this study was strongly believed to be due to the settings under which these tests were conducted. This argument is particularly valid to poor air

distribution. Although the overlap of combustion phases is common in biomass (Claar et al., 1980), poor air distribution in these tests resulted in substantial overlap of the first two phases and to a lesser degree of the three. In all runs, wafers facing the main air stream burned earlier and more intensely throughout the combustion process. The flames and energy thus generated were used to heat up other wafers causing moisture evaporation, flaming and, in some cases later in the process, glowing combustion simultaneously.

It was also noticed on several occasions that some wafers away from the main air stream initiated but failed to sustain combustion although those facing the air stream were undergoing intense combustion. It was likely partially due to the quenching effect of the endothermic moisture evaporation they were still experiencing. This may be another indication of the seriousness of the overlap occurred during these tests. Consequently, the detection of moisture evaporation as a distinct initial phase was rather difficult. In other words, moisture evaporation was taking place throughout the combustion process.

As for stack temperature, T_s, data showed that, in all cases, it was only slightly lower than flame temperature almost throughout the flaming combustion phase. This was a clear indication that both elephantgrass and energycane produced high flames when burned as was evidenced by the fact that the T_s probe was more than 150 mm above the T_f probe. The high flames were suspected to be due to the high volatile content of both materials as can be seen from Table (6-1). During the char combustion

phase, T_s fell almost at the same rate as T_f but was consistently but not substantially lower (5 to 15%) than the flame temperature as evident in Figs. (6-2) and (6-3).

The high stack temperature compared to flame temperature was attributed on the one hand to the high flames produced and to the measurement of both temperatures inside the small stove on the other. This was confirmed when the temperature data at the end of the stack was examined. It showed a significant difference between the flame and stack temperatures. Nonetheless, the data generally indicated that a significant amount of energy was lost with exhaust gases that it merits investigating potential uses of that energy. In fact, in some similar applications, all the energy utilized was the heat energy taken away with the flue gases. That energy was used in such applications as heating, steam generation and drying (Singh et al., 1980).

For both materials, flame combustion lasted shorter than glowing combustion. Observations implied that glowing combustion of wafers started at the outer surface and proceeded inward. Moreover, in all runs, it was found that toward the end of combustion a small portion of each wafer was left partially unburned and were characterized as hard to burn. These small portions were believed to be the cores of wafers, which were probably the hardest and densest part of the wafer and thus were hard to oxidize. However, their proportions did not appear to bear any significant consequences.

Effectiveness of Insulation

The purpose of installing firebrick on the inside walls of the stove was to measure the effectiveness of fire brick insulation in impeding heat loss through the walls of the stove to the surroundings. Data for the insulation temperature, T_i, measured at the outer surface of firebrick, showed that it followed a profile similar to that of flame and stack temperatures. It increased gradually from its pre-combustion temperature to a peak value and then smoothly declined to a steady state value as shown in Fig. (6-4) below. However, it was noticed that it took the insulation temperature twice as much time to reach a maximum temperature that was only 10 to 20% of maximum flame and stack temperatures.

The observations mentioned above indicated that a significant time lag existed between the maximum T_i and the corresponding maximum flame and stack temperatures. It was interesting to notice that in all runs the insulation temperature reached a maximum almost precisely at the time T_f and T_s first reached their lowest levels toward the end of the burning process, which accounted to about 70% of the total burning time.

To carry the analysis a step further, a quantitative assessment of heat loss by conduction was carried out (Appendix C). The calculations were based on the assumptions of perfect combustion, steady one-dimensional heat flow, a steady temperature of 500 C and 45 C for the inner and outer walls, and a 1 kg/hr feed rate. The results indicated that heat loss from the stove due to conduction with insulation

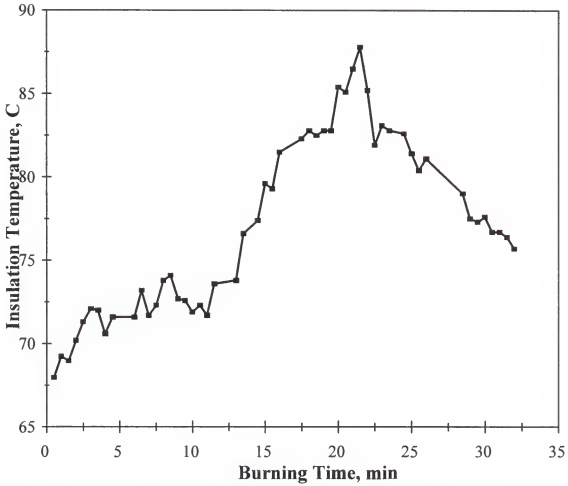

Fig. 6-4. Variation in temperature of brick insulation during wafer combustion.

was only 1.34% of the total heat input into the furnace. It was clear that this number would be much larger if the insulation material did not exist. This was supported by the fact that the thermal resistance of the brick used was more than 225 times that of the stove steel outer cover.

These results indicated that the conduction heat transfer through the brick was very slow and the material possessed poor heat conduction characteristics. Hence, it

may be concluded that, in such applications, the insulation was not only effective but also necessary. Huff (1980) studied burning wood cubes and confirmed the essential need for refractory to minimize heat loss and maintain a high temperature in the fire box, which enhanced the combustion process.

Stove Performance

The stove performance was studied by attempting an approximate estimation of its efficiency. Due to a lack of reliable and sufficient data on the actual combustion process, the stove performance was evaluated assuming complete combustion of 1.0 kg of elephantgrass. The stove efficiency was defined as the proportion of total heat released that would stay within the stove and be utilized under the conditions of a continuous and steady burning process. It may be expressed as

$$\eta_s = \frac{TotalHeatInput - Losses}{TotalHeatInput} \qquad (6\text{-}1)$$

where η_s = stove efficiency (%).

The total heat input was simply the heating value of the fuel, which was in this case about 17250 kJ/kg is the "as received" heating value of elephantgrass (see Table 6-1). The losses included heat energy lost due to moisture evaporation, heat conduction, and the heat carried away with dry exhaust gases.

The heat loss due to moisture evaporation was determined based on the rationale that the moisture would be heated from ambient conditions (its condition when it was introduced into the stove) to the boiling point of 100 C and then superheated to the

temperature of exhaust gases. According to the data collected, a steady stove and exhaust temperatures of, respectively, 500 C and 300 C were assumed. The ambient temperature, T_a, and ambient pressure, P_a, were set (measured) at 30 C and 1 atm.

The heat loss due to moisture evaporation was divided into two parts. The first was due to moisture in the material (15%, w.b.) and the second was due to the oxidation of the material hydrogen into water. Calculations showed that the first part accounted for 2.33% heat loss of the total heat input compared to 6% for the second. The latter larger loss was due to the fact that 1.0 kg of material hydrogen would produce 9 kg of water when oxidized. Heat loss due to conduction through the stove walls was presented in the previous section and accounted for 1.34%.

The sensible heat taken away with flue gases, Q, was determined according to the formula

$$Q=m_g c_p \Delta T \tag{6-2}$$

where m_g is mass of dry flue gases per Kg of material

c_p is the overall (mixture) specific heat of flue gases, kJ/kg K

ΔT is the temperature difference between flue gases and ambient air

The quantity of flue gases, m_g, was equal to the total products of complete combustion, including excess air, less the ash and water vapor (see Table 6-3). The overall specific heat, c_p, was calculated assuming that the combustion products made a mixture of ideal gases.

It was found that the heat energy lost with the flue gases was approximately 25% of the total energy input, which is equivalent to more than 72% of the total heat loss. This substantial quantity of lost energy was expected earlier due to the high temperature at which the flue gases left the stove. A detailed description of the methodology of carrying out these calculations is presented in Appendix (C).

Based on these calculations, the stove efficiency, from Eqn. (6-1), was approximately 65%, which was in general higher than those reported in the literature in similar applications. This was attributed mainly to assuming perfect combustion of the material. The actual process would involve partial oxidation of combustible components, particularly carbon, and would leave some unburnt combustibles in the residue, both would result in less heat release. Consequently, the efficiency of the stove would be less than 65% depending on the degree of incompleteness of combustion.

Although the assumption of complete combustion had an important bearing on the high stove efficiency, it should be born in mind that the comparison made above may be questionable or even invalid. This was because a universally accepted standard procedure as to the definition of stove efficiency under small-scale settings was not found. Instead, different workers defined stove efficiency based on the portion of combustion heat that was to be utilized, which in turn depended on the intended end use of the stove such as cooking, heating....

Ash Analysis and Slagging Potential

Ash analysis is the principal means and forms the basis for evaluating the slagging potential of biomass materials and is a part of the chemical analysis of fuel materials. The results of ash analysis of elephantgrass and energycane is shown in

Table (6-6). Ash analysis of elephantgrass and energycane. All values are averages of three samples.

Element	Elephantgrass	Energycane
Ca	0.18133	0.15267
Mg	0.10260	0.13533
K	0.83433	0.47133
P	0.18067	0.08453
Na	0.02930	0.99397
Si	0.03460	0.04387
Zn	0.00367	0.00135
Cu	0.00039	0.00013
Mn	0.00647	0.00763
Al	0.00327	0.00217
Fe	0.00614	0.00372

Table (6-6). The values in the Table (6-6) are reported as percent of material dry matter (DM). For instance, K and Na for energycane are 0.47133 and 0.99397, which means that the two elements made up 0.47% and 0.99% of DM, respectively.

According to the combustion tests carried out in this study, both materials showed essentially no signs of slagging. It is a well established fact that as long as the furnace temperature is below the slagging temperature of the fuel material, slagging signs will not appear. For this reason, the absence of slagging in this study was attributed primarily to the low stove temperature (a maximum of about 500 to 550 C) that was far below the slagging temperature of these materials. The slagging temperature of elephantgrass was estimated in the range of 900 to 1000 C (Tuhoy and Juhasz, 1994). The corresponding temperature for energycane is not expected to deviate significantly from that of elephantgrass.

Should these materials be utilized in large-scale applications and/or at higher feed rates for extended time periods (higher temperatures), their slagging potential is best evaluated by calculating their slagging (fouling) index (lb Alkali/MMBtu). This index is determined by the formula

$$\frac{100}{HHV(Btu/lb(dry))} * Ash\% * Alkali\%ofAsh = \frac{lbAlkali}{MMBtu} \qquad (6\text{-}3)$$

where HHV is the material higher heating value. The Alkali% is defined as the sum of percent potassium oxide, K_2O, and sodium oxide, Na_2O in the ash. It may be expressed as follows:

$$Alkali\% = \%K_2O(ofash) + \%Na_2O(ofash)$$

Provided that all elemental potassium, K, and sodium, Na, in the material was converted into their respective oxides upon ashing (burning) and that all K and Na recovered in the ash analysis was obtained from these oxides, the fouling indexes for elephantgrass and energycane were estimated from Eqn. (6-3) to be 0.900 and 0.789, respectively.

According to Miles et al. (1993), elephantgrass fell in the category of biomass materials that would cause "certain slagging" (slagging index $>$ 0.80) while energycane was favorable and fell in the range of "probable slagging" (slagging index $<$ 0.80).

For cane type materials, Jenkins et al. (1994) indicated that potassium was a major fouling agent. The potassium content in energycane was about 56% of that in elephantgrass (see Table 6-6) and was obviously reflected in their fouling indexes. A material having a slagging index less than 0.40 is characterized as having a "minimal" slagging potential. In this range, only soft and loose deposits are formed that soot blowers can remove. Higher slagging indexes imply serious deposit formation that are unmanageable without substantial efforts.

It should be emphasized that the figures for fouling indexes presented above should be viewed as rough estimates and should not be used for accurate calculations. This is mainly due to assuming that all elemental K and Na was converted to oxides,

which would introduce an error in calculating the %Alkali in ash (Eqn. 6-3). The degree of error would depend primarily on the chlorine content in materials that would result in converting part of these elements to other compounds, especially salts, instead (Jenkins et al., 1994). This applies in particular to potassium, the oxides of which in these calculations made up more than 90% of the total %Alkali in ash. Appendix B presents additional details on calculating the slagging indexes of both materials.

It is noteworthy, though, that the range of slagging temperature for these materials is high compared to the range for biomass in general, which was estimated at 650 to 750 C (Miles, 1992). Consequently, elephantgrass and energycane possess an important advantage over other biomass materials in this regard. The reason for this is that, when these materials are burned, stove or furnace temperature can reach as high as 900 to 1000 C before fouling (slagging) is initiated as compared to 650 to 700 C for other biomass.

The bottom line is then, the suitability of these materials as fuel from a slagging viewpoint is determined primarily based on the maximum fire box temperature required for a given application. It is clear that small-scale applications involve less feed rates, intermittent use and in many cases lower temperatures in comparison to large-scale applications and may, therefore, be utilized successfully in such applications.

Combustion vs. Compression Conditions

Under all densification conditions, wafers of both materials burned satisfactorily once ignited. However, the compaction conditions seemed to influence the behavior of

wafers while burning. All wafers expanded (swelled) to varying degrees while burning although they all maintained their shape and integrity throughout the process. Tests of both materials showed that the product made in the smallest die (40 mm) under high pressure (37 MPa) experienced the least expansion while those made in larger dies and/or at lower pressures tended to expand more during combustion. Moreover, the smallest wafers burned efficiently producing the highest maximum flame temperature and the longest burning times.

It was clear that expansion or swelling initiated a breaking apart process that exposed more of the material to oxidation and resulted in an increase in mass consumption rate and thus shorter burning times. Furthermore, since all runs were made with the same total mass, the smallest wafers had more total surface area exposed to combustion air and, thus burned more efficiently than larger ones. This added another favorable characteristic to smaller wafers, which were more durable than larger ones as was shown in previous chapters.

Examining the chemical and energy analyses of materials showed only slight differences in almost all aspects. Accordingly, a comparison of the two materials indicated that elephantgrass wafers were slightly favorable to those made from energycane. Maximum flame temperature achieved by the former was in the range 480 to 580 C while the latter attained a range of 425 to 500 C. This result was expected as it was most likely due to the higher calorific value of elephantgrass. Additionally, energycane wafers expanded generally more and burned for shorter times. Furthermore, energycane wafers produced more ash than elephantgrass wafers. This

can be explained by examining the ash content of both materials, which shows that energycane ash content is apparently higher than elephantgrass.

CHAPTER 7
CONCLUSIONS AND RECOMMENDATIONS

This study involved a systematic assessment of the potential of two biomass materials, namely, elephantgrass and energycane, as a source of energy. Both materials were compressed to form small compact units called wafers, which were tested under conditions typical of those that exist under small-scale applications. In the process, a review of relevant literature, the characteristics of material compaction and their combustion characteristics were addressed. This chapter provides a brief summary of the major findings as related to the aspects covered in the study.

Despite the fact that these same materials were burned under different settings, mainly in large-scale applications, the literature indicated that the materials were used in the unconsolidated state and caused several serious difficulties and problems. Some of the problems were common to both large- as well as small-scale applications.

Most of the problems were attributed to the inherently low bulk density of these materials. The compaction of the material resulted in significant improvement in those problem areas. For example, significant increases in material bulk density associated with proportional increases in material energy density and reductions in material volume in addition to better handlability were realized. Increases in material bulk

density ranged from 4 to 9 times while a range of at least 6.5 to 10.0 of volume reduction was achieved.

In evaluating the feasibility of biomass bulky materials as a potential fuel, transportation and storage costs come into play as major factors. The increase in material density and reduction in its volume resulted from compaction are translated into proportional savings in material transportation and storage costs and, thus, provide a better chance for these materials to compete in the energy market.

Material compaction constitutes an upgrading process due to the many benefits associated with the material consolidated form. However, this upgrading is brought about at a cost. Knowledge of energy requirement for material compression is another important consideration in studying the feasibility of these materials as an energy source. The energy required for compressing elephantgrass and energycane was obtained by calculating the area under the stress-deformation curves and covered a wide range from 12 to 50 MJ/ton in direct proportionality to the stress level applied and die diameter. These ranges constituted a small fraction of the calorific value of either material and did not exceed 0.30% of their energy content, which compares favorably with many other biomass materials.

The functional and structural design of sound compression machines and processes require a knowledge of material compression mechanics such as stress-deformation and stress-density relationships. Density is the most important physical characteristics of the final product for it is a major factor in realizing many of the benefits of material compaction and determining the quality of the final product.

Like many other biomass materials, the stress- deformation and stress-density relationships of elephantgrass and energycane assumed an exponential form as follows

$$\sigma = c_0 10^{c_1 y} \tag{7-1}$$

where σ is the stress at any time during compaction

y stands for the deformation or density of material at any time during compression

c_0 and c_1 are parameters

It can be seen from Eqn. (7-1) that a knowledge of the satisfactory range of product density determines the level of stress required. The latter has profound consequences on the energy required, compaction machine design and the optimization of the process. However, the form of Eqn. (7-1) entailed a few shortcomings in describing the relationship between stress and material deformation and density. A better expression of the stress-density relationship was

$$\frac{\rho_{max} - \rho_i}{\rho_{max} - \rho_0} = c_0 - c_1 \log(\sigma) \tag{7-2}$$

where α and γ are parameters

$\rho_{max.}$, ρ_i, ρ_0 refer to maximum, instantaneous and initial density, respectively. The product maximum density, expressed here as the product immediate density, ρ_{max}, is of particular importance. Therefore, a prediction equation was developed for ρ_m in terms of the relevant process and material variables.

After wafers are made with the intention to be evaluated as a potential fuel, there are two aspects that need be investigated, namely, their quality and their combustion characteristics. Wafer quality is expressed in terms of two criteria: stability and durability. Since wafer final density, ρ_f, is of most practical interest and is directly proportional to changes in product physical dimensions, it was used as the criterion to express wafer stability. Linear regression was utilized to develop adequate model equations to predict ρ_f in terms of the relevant machine, process and material variables for both materials. Dimensional analysis proved to be a useful tool in realizing a compact model for elephantgrass.

In this study, wafering conditions (P_{max}, D_c, t_h) were the major variables of material compaction. The response of the two materials to P_{max} was different. The quality of elephantgrass wafers was more favorable than those of energycane at all P_{max} levels except at the highest levels (37 and 58 Mpa) in the 40-mm die. This difference was primarily due to the larger stem proportion of energycane and its higher crude protein content.

For the two materials, a 5-sec hold time was considered an optimum. As for D_c, the two larger dies (63- and 76-mm) failed to produce wafers of acceptable quality, which was attributed to more severe impact and shearing forces in the subsequent handling of larger wafers and/or their lower final density. In the two smaller dies (40- and 50-mm), the range of final density for good quality was 290 to 320 kg/m^3, which corresponded to an immediate density range of 400 to 420 kg/m^3 to account for wafer

expansion. In these dies, a range of 17 to 24 MPa was a sufficient minimum to produce this range of wafer density.

The combustion tests conducted on wafers using 70 to 80% excess air indicated that they possessed poor ignition quality but once ignited, they burned satisfactorily to the end. The theoretical air requirement for elephantgrass and energycane were 5.39 and 5.14 kg air per kg material, respectively. The tests also showed that wafers burned in two distinct stages, specifically, an intense flaming combustion phase followed by a slower char combustion phase. The absence of a distinct initial moisture evaporation phase was principally attributed to poor air distribution, which caused serious overlapping of this phase with the other two.

The metal stove used was evaluated as to its efficiency, η_s, which was defined as the ratio of heat that was retained inside the stove to the total heat input. The formula used was

$$\eta_s = \frac{TotalHeatInput - Losses}{TotalHeatInput} * 100 \qquad (7\text{-}3)$$

The losses included those due to the evaporation of material moisture, which included the moisture formed due to the oxidation of material hydrogen and material moisture, heat loss due to conduction and the sensible heat carried away with dry flue gases. The resulting stove efficiency was about 65% and the major losses were due to the heat carried away with flue gases. Furthermore, an assessment of the effectiveness of the brick insulation indicated that it was very important if heat losses were to be minimized.

According to the combustion tests carried out in this study, no slagging signs were noticed, which was clearly a result of the fact that the maximum stove temperature was far below the fusion temperature of these materials. However, due to the limited scale of the tests, conclusive decisions could not be made in this regard. Ash analysis provided the information required to evaluate the materials slagging potential, expressed in terms of a slagging index, should the materials be burned at higher feed rates for extended periods of time.

It was roughly estimated that the slagging (fouling) indexes of elephantgrass and energycane were 0.900 and 0.788, respectively. According to these relatively high indexes, elephantgrass and energycane fall in the "certain" and "probable" slagging regions, respectively. However, their high fusion temperature compared to many other biomass materials gives them an advantage in this regard, especially in small-scale applications.

Further research is required in the following areas

1. The inclusion of other parameters in studying material compaction including maturity stage, particle size, material and/or die heating (temperature), and biomechanical properties.

2. Investigating the potential of utilizing artificial binders in improving wafer adherence and quality.

3. The influence of a better more uniform air distribution system on material combustion.

4. Studying the possibility of an automated feeding system. The compact form of material lends itself readily to such a possibility and makes the materials more attractive to use.

5. Examining the possibility of upgrading these materials by mixing them with other biomass-based (wood) or fossil fuels (coal).

6. A comprehensive economic appraisal of compressing and utilizing these materials as fuel.

APPENDIX A
THE Π-TERMS OF ELEPHANTGRASS FINAL DENSITY MODEL

The dimensional analysis technique was applied using the Buckingham pi theorem. The functional relationship between the dependent variable, ρ_f, and the independent variables was given by

$$\rho_m = f(\rho_m, t_h, P_{max}, D_c, X_{max}, MC, W, H) \quad \text{(A-1)}$$

Due to the absence of thermal effects, the primary dimensions were limited to mass (M), length (L), and time (T). The repeated variables selected were W, m, and Dc . Three variables were chosen since the largest square matrix of nonzero determinant was 3 by 3. The dimensional matrix of this problem is shown in the following table

	ρ_f	ρ_m	t_h	P_{max}	D_c	X_m	MC	W	H
M	**1**	1	0	1	**0**	0	0	**1**	0
L	**-3**	-3	0	-1	**1**	0	0	**1**	1
T	**0**	0	1	-2	**0**	0	0	**-2**	0

To ensure that these three variables were linearly independent, as required by the theorem, the 3 by 3 matrix consisting of the rows and columns of the three repeated

variables was constructed (shown in boldface in the table) and its determinant was determined. It turned out that the determinant was different from zero, and thus the condition of linear independence was met.

Now, for the ith π, we construct π^*_i in terms of the variable x_i as

$$\pi^*_i = x^*_i (x^*_1)^a (x^*_2)^b (x^*_3)^c \qquad \text{(A-2)}$$

where any variable with an asterisk (*) refers to that variable in absolute size

x_1, x_2, x_3 are the repeated variables

a, b, c are exponents with values that make Eqn. (2) non-dimensional

For any variable, say x_i,

$$x^*_i = x_i (P_1)^d (P_2)^e (P_3)^f \qquad \text{(A-3)}$$

where P_1, P_2 and P_3 are the primary dimensions

d, e, f are the appropriate exponents depending on the dimensions of x_i

Substituting Eqn. (A-3) for each variable in Eqn. (A-2), we get the first pi term.

Applying this approach to this problem and starting with ρ_f, for instance, we have

$$\pi_1 M^0 L^0 T^0 = \rho_f \, ML^{-3} \, (D_c L)^a \, (WMLT^{-2})^b \, (\rho_m ML^{-3})^c$$

Equating the exponents of each primary dimension on both sides of Eqn. (4) gives

M exponent: $1+b+c = 0$

L exponent: $-3+a+b-3c = 0$

T exponent: $-2b = 0$

Solving the last three equations simultaneously gives

$$b=0$$

$$a=0$$

$$c=-1$$

which yields

$$\pi_1=\frac{\rho_f}{\rho_m}$$

In a similar fashion, taking each remaining variable in turn, together with the 3 repeating variables produces the required six nondimensional variables. Notice that the total number of nondimensional variables should be the total number of variables (nine, in this case) less the number of repeating variables (matrix rank).

APPENDIX B
AIR REQUIREMENT AND MASS BALANCE OF MATERIALS

In chapter 5, tables were developed to determine the theoretical air requirement for the complete combustion of both elephantgrass and energycane and to perform mass balance on the reactants and products of combustion. This Appendix introduces the details of the methodology used in performing those calculations.

Air Requirement

In order to calculate the air required, the amounts of required oxygen, O_2, to completely oxidize the combustible components must be determined. The amount of nitrogen, N_2, is determined by a knowledge of air composition. The material ultimate analysis provides the information needed as to the mass proportions of the components C, H_2, O_2, N_2, S and H_2O in the material. A knowledge of the molecular weight (MWt) of each component makes it routine to convert these into moles. Based on a balanced chemical reaction of the combustible components, the amount of O_2 require for each component is determined.

It is assumed that only C, H_2, and S will undergo an oxidation reaction to produce carbon dioxide, water and sulfur dioxide as follows:

$$C+O_2 \rightarrow CO_2$$

$$H_2+\frac{1}{2}O_2 \rightarrow H_2O$$

$$S+O_2 \rightarrow SO_2$$

It can be seen from these reactions that the ratio of the number of moles of O_2 required for the complete oxidation of C and S is 1:1 and that for H_2 is 0.5:1. Consequently, the total amount of O_2 required to burn the combustibles in the material is simply the sum of O_2 required for the oxidation of those components. However, since the material itself contains O_2, the net amount in moles of O_2 required is the sum obtained above less the material O_2.

To obtain the amount of N_2 that will enter with the combustion air, it is assumed that the latter is composed of O_2 and N_2. Since the molar ratio of air N_2 to O_2 is 3.76, the amount of N_2 is equal to the required O_2 multiplied by 3.76. The amount of air required is, then, obtained by converting the moles of O_2 and N_2 (air) to mass units as follows:

(moles of O_2)(MWt of O_2) + (moles of N_2)(MWt of N_2)

The molecular weight of O_2 is 18 kg/kmole and that of N_2 is 27 kg/kmole.

Mass Balance

As for mass balance of the inputs and outputs of combustion, it is obvious that the output will include CO_2, H_2O and SO_2 as shown in the reactions above. Additionally, N_2 and H_2O will leave unoxidized as part of the combustion products. It can be seen from the reactions above that the molar ratio of all the reacting components to their corresponding products is 1:1. The components CO_2 and SO_2 are determined directly from the known amounts of C and S, respectively. In contrast, the total amount of H_2O will include the material moisture that leaves as is and the water formed from the oxidation of material hydrogen. As for N_2, it is the sum of material N_2 and the amount that entered with the combustion air calculated earlier.

When the mass balance is performed, the mass of the reactants must be equal to the mass of combustion products so that the principle of conservation of mass is satisfied. This was demonstrated in the tables presented in the text.

APPENDIX C
DETERMINATION OF HEAT LOSSES FROM THE STOVE

In calculating the stove efficiency in chapter 6 on material combustion, several heat loss sources from the stove were calculated and presented as percentages of total heat input into the stove. The sources of heat loss included conduction, moisture evaporation, and heat taken away with flue gases. This appendix provides an illustration of the methodology utilized in calculating each type of loss.

Heat Loss by Conduction

The heat lost from the stove to the surroundings by the conduction of heat through stove walls is given by

$$q_c = \frac{\Delta T}{\Sigma R_t} \qquad \text{(C-1)}$$

where q_c is the rate of heat loss per unit area

ΔT is temperature difference across stove walls

ΣR_t is the total thermal resistance of stove wall

The last two terms were determined based on the data collected and material properties:

Temperature difference, ΔT. This term was calculated based on an inside stove (wall) temperature of 500 C and an outside wall temperature of 45 C.

Total thermal resistance, ΣR_t. Recall that stove walls consisted of an internal brick liner and a steel sheet arranged in series. They were 0.03175 and 0.00635 m thick, respectively. By definition, for a material

$$R_t = \frac{x}{kA} \qquad \text{(C-2)}$$

where x is the wall thickness

k is the thermal conductivity of wall material

A is the wall area (0.09 m^2)

From heat transfer tables, the thermal conductivity, k, for brick and steel was 1.0 and 45 w/m C, respectively. Since the materials were arranged in series, the total thermal resistance is the sum of their resistances, or,

$$\Sigma R_t = R_{t_b} + R_{t_s} \qquad \text{(C-3)}$$

Substituting these values in Eqns. (C-1) and (C-2) above, it was calculated that the heat conduction from stove walls was

$$q_c = 230 \text{ kJ/hr}$$

This quantity made 1.34% of the total heat input in the stove. The latter was about 17250 kJ/kg, which is the heating value of the material from energy analysis.

Heat Loss Due to Moisture Evaporation

This loss included both the material moisture and that formed due the oxidation of material hydrogen.

Loss Due to Material Moisture, q_1. Based on the rational mentioned in the text, heat lost due to material moisture evaporation is given by

$$q_1 = MC[(100 - T_a) + h_{fg} + C_{pm}(T_s - 100)] \qquad \text{(C-4)}$$

where MC is the amount of moisture/kg material (0.15)

T_a is the ambient temperature (30 C)

T_s is the temperature of flue gases in the stack (500C)

h_{fg} is the heat of vaporization of water (2257kJ/kg)

C_{pm} is the specific heat of water (1.95 kJ/Kg K)

Plugging these values in Eqn. (C-4), it turned out that

$$q_1 = 407 \text{ kJ/kg}$$

which was 2.33% of the total heat input.

Heat Loss Due to Oxidation of Material H_2, q_2. From a balanced oxidation reaction of hydrogen, it is routine to show that 1 kg of hydrogen yields 9 kg of water. The formula used for this type of loss was

$$q_2 = (9H - MC)[(100 - T_a) + h_{fg} + C_{pm}(T_s - 100)] \qquad \text{(C-5)}$$

Substituting the values in Eqn. (C-5) yields

$$q_2 = 1036 \text{ kJ/kg}$$

which made 6% of the total heat input. The total heat loss due to moisture evaporation is the sum of q_1 and q_2.

Heat Carried Away with Dry Flue Gases, Q

This type of loss is the sensible heat carried away with the products of combustion including excess air and is given by

$$Q = m_f C_{pf} \Delta T \qquad \text{(C-6)}$$

where m_f is the mass of dry flue gases

C_{pf} is the specific heat of the mixture of gases

ΔT is the temperature difference between flue gases and ambient air (470 C)

Mass of flue dry gases, m_f. This term is calculated from the mass balance tables in Ch. 6. From Table (6.3), 1 kg material would produce 1.672 kg CO_2, 4.1413 kg N_2, and 0.0016 kg SO_2 in addition to 2.2216 kg excess air. Ash and water should be excluded. This adds up to give

m_f = 8.0365 kg of dry products/kg material.

Specific heat of gases, C_{pf}. Assuming that the combustion products make a mixture of ideal gases

$$C_{pf} = \Sigma y_i C_{p\,i} \qquad \text{(C-7)}$$

where Cp_i the specific heat of each individual component of the products

y_i stands for the mass fraction of each individual component and defined for

component *i* as follows:

$$y_i = \frac{m_i}{m_f} \tag{C-8}$$

The values y_i are calculated and Cp_i are pulled out from the tables of thermodynamics. Accordingly, it was found that

$$C_{pf} = 1.119 \text{ kJ/kg K}$$

Substituting in Eqn. (C-6) gives

$$Q = 4230 \text{ kJ/kg}$$

This amount accounts for approximately 25% of the total heat input into the stove.

Summing up all types of losses with the heat input being known, the stove efficiency was calculated.

APPENDIX D
CALCULATION OF SLAGGING INDEXES

The slagging or fouling index is a figure that was originally developed to evaluate the fouling potential of coal. It proved to be a very useful tool to evaluate various biomass fuel materials. Based on this figure, biomass materials can be roughly classified in regard to their slagging potential.

In principle, determining the slagging index involves calculating the weight in pounds of alkali (K_2O + Na_2O) per million Btu (MMBtu) in the fuel. The formula used for calculating the alkali is the following:

$$\frac{lbAlkali}{MMBtu} = \frac{10^6}{Btu/lb(dry)} * Ash\% * Alkali\%oftheAsh \qquad \text{(D-1)}$$

The result from Eqn. (D-1) must be divided by 10,000 to get the final correct number used in calculating the slagging index.

The terms Btu/lb and Ash% in materials (Eqn. D-1) are readily available from energy and chemical analyses. The last term on the right-hand side of Eqn. (D-1) is determined utilizing data provided by the ash analysis, which is presented in detail in table format in the text (see Table 6-6).

Slagging Index of Elephantgrass

From the material report of analysis, it was found that

$$\text{Ash}\% = 2.63$$

$$\text{Btu/lb (dry)} = 8112.0$$

Thus, we are left with determining the first term in Eqn. (D-1). The ash analysis involved ashing 1.5 g of material dry matter, which was digested in a 15-ml acidic solution. It was found from the ash analysis that the 1.5 g dry matter contained 0.04 g ash. The results of analysis indicated that elephantgrass samples contained an average of 581.5 mg K/liter. Therefore, in order to get mg K per kg ash, X_1, we may write

$$(581.5 mgK/L)(15 ml/1.5 gDM)(1.5 gDM/0.04 gash)(1L/1000 ml)(1000 g/kg) \qquad \text{(D-2)}$$

The result is

$$X_1 = 218062.5 \text{ mg K/Kg ash}$$

To convert the last figure to mg K_2O/kg ash, Y_1, which is the first part of alkali, we write

$$(X_1)(1 mmoleK/39 mgK)(1 mmoleK_2O/2 mmoleK)(94 mgK_2O/1 mmoleK_2O)$$

The result is

$$Y_1 = 262793.27 \text{ mg } K_2O/\text{kg ash}$$

This result was obtained by assuming that all K in the material was converted into K_2O upon ashing and that all K recovered in the ash analysis was coming from that

compound. To express Y_1 in (%), it must be divided by 10,000, which yields

$$Y_1 = 26.28\% \ K_2O$$

As for sodium oxide (Na_2O), the second part of alkali, elephantgrass samples contained an average of 29.3 mg Na/liter. Following the same steps as for K, it turned out that

$$X_2 = 10987.5 \text{ mg Na/kg ash}$$

from which, it was found that

$$Y_2 = 14809.24 \text{ mg Na2O/kg ash}$$

which is equivalent to

$$Y_2 = 1.48\%$$

Therefore, the % alkali in ash = Y1(%) + Y2 (%)

$$= 27.76\%$$

Substituting all the values in Eqn. (D-1) and dividing by 10,000, gives for elephantgrass

$$\text{Slagging Index} = 0.900$$

A similar procedure using the relevant data of energycane gives

$$\text{Slagging Index} = 0.788$$

As indicated earlier, the value of the slagging index of a material reveals much about its fouling potential. In particular, a material having a slagging index less than 0.40 is characterized as having a "minimal" slagging potential. In this range, only soft and loose deposits are formed where soot blowers are sufficient to remove them. A slagging potential in the range of 0.40 to 0.80 implies the material has a "probable"

slagging potential and a slagging potential above 0.80 means the material has a "certain" slagging potential. Higher slagging indexes involve serious deposit formation that are unmanageable without substantial efforts.

APPENDIX E
STATISTICAL ANALYSIS

Statistical analysis is a powerful tool in the analysis and interpretation of experimental data. The statistical software package SAS was used exclusively in all the analyses conducted in this study. In particular, the procedures of regression (PROC REG), general linear model (PROC GLM) and sorting (PROC SORT) were of special relevance. These procedures were used in developing prediction equations of wafer density, which is the single most important physical characteristic of densified biomass. The procedures were also utilized in studying the influence of hold time on wafer density and its interactions with other relevant variables.

Wafer Immediate Density

In chapter 4, a prediction equation was developed for the wafer immediate density, ρ_m, of both materials. A first-order linear regression model was proposed to relate the dependent variable, ρ_m, to the independent variables as follows

$$\rho_m=\beta_0+\beta_1 t_h+\beta_2 P_{\max}+\beta_3 D_c+\beta_4 MC+\beta_5 W+\beta_6 \rho_0+\varepsilon \qquad \text{(E-1)}$$

The parameters β_i (I=0, 1, ..., 6) were determined using either the GLM procedure or

the REG procedure. The code for the first procedure looks typically like the following:

```
DATA [DATA NAME];
INFILE '[PATHNAME]';
INPUT [LIST OF ALL VARIABLES];
RUN;
PROC GLM DATA=[DATA NAME];
CLASS [LIST OF CLASS VARIABLES];
MODEL [DEPENDENT VARIABLE]=[LIST OF INDEPENDENT VARIABLES];
MEANS [VARIABLE]/TUKEY;
RUN;
```

The code for PROC REG is very similar except that a CLASS statement can not be used. In fact both procedures yield quite similar outputs.

The user should enter the information between brackets. The class statement lists the variables that have discrete non-continuous values or levels. In this study, P_{max} (4 levels), D_c (4 levels) and t_h (3 levels) were the class variables. The Tukey procedure is a well-known multiple comparison technique.

For the sake of illustration, the output from the PROC GLM for the immediate density of energycane is shown in the table below. The value of R_d^2 was about 0.91. A similar output was obtained for elephantgrass with an R_d^2 value of about 0.88.

Wafer Final Density

In chapter 5, prediction equations were developed for the wafer final density, $\rho_{f,}$ of both materials. As an example, the SAS output for elephantgrass was inserted in the body of text in that chapter. The procedure is similar to that utilized for the immediate density. The table below shows the corresponding output for energycane.

Table (E-1). The general linear model procedure for the prediction equation of ρ_m of energycane.

Source	DF[a]	SS[b]	MS[c]	F value
Model	11	3422479.1	311134.5	246.04
Error	238	300972.9	1264.6	
Corrected Total	249	3723452.0		

Source	DF	Type III SS[d]	MS	F value	Pr>F
t_h	2	8985.7	4492.9	3.55	0.0001
P_{max}	3	4449888.2	149962.7	118.59	0.0001
D_c	3	150026.7	50008.9	39.55	0.0001
MC	1	107612.4	107612.4	85.10	0.0001
W	1	14539.0	14539.0	11.50	0.0008
ρ_0	1	15203.4	15203.4	12.02	0.0006

Parameter Estimates

Variable	DF	Estimate	SE[e]	T for H_o[f]	Prob>|T|[g]
Intercept	1	1187.33	48.80	24.3	0.0001
t_h	1	-1.38	0.64	-2.16	0.0316
P_{max}	1	5.19e-6	2.9e-7	17.91	0.0001
D_c	1	-14495	1497.67	-9.68	0.0001
MC	1	-25.92	2.09	-12.38	0.0001
W	1	18.80	4.31	4.36	0.0001
ρ_0	1	0.39	0.065	6.04	0.0001

[a] DF stands for degrees of freedom

[b, c, e] SS, MS and SE stand for sum squares, mean squares, and standard error

[d] For unbalanced data entries at each level of P_{max} and D_c, type III SS had to be used

[f] H_o is the null hypothesis defined as H_o: $\beta_i=0$

[g] Since the value of $\alpha=0.05$, a parameter is significant if this value is greater than 0.05

Table (E-2). The general linear model procedure for the prediction equation of ρ_f of energycane

Source	DF	SS	MS	F value
Model	8	3565051.3	445631.42	649.0
Error	241	165481.8	686.65	
Corrected Total	249	3730533.1		

Parameter Estimates

Variable	DF	Estimate	SE	T for H_o	Prob > |T|
Intercept	1	-1414.10	124.8	-11.3	0.0001
t_h	1	1.62	0.47	3.49	0.0006
P_{max}	1	1.40e-6	2.80e-7	4.927	0.0001
D_c	1	223376.0	1801.09	12.42	0.0001
X_{max}	1	-1.44	0.154	-9.36	0.0001
ρ_m	1	1.71	0.093	18.53	0.0001
W	1	-40.30	3.42	-11.79	0.0001
H	1	29338.0	2311.52	12.69	0.0001
MC	1	-2.32	1.61	-1.44	0.1517

Influence of Hold Time on Wafer ρ_f

It was pointed out that due to the inconsistency of the influence of hold time on ρ_f, the hold time had to be investigated at fixed levels of P_{max} and D_c. The inconsistency was attributed to highly significant interaction among the three variables, which statistically proved to be true.

In such cases, the procedure PROC SORT along with the other procedures is of prime importance. The code used for this case was

```
DATA [DATA NAME];
INFILE '[PATHNAME]';
INPUT [LIST OF ALL VARIABLES];
RUN;
PROC SORT [DATA=DATA NAME];
 BY [LIST OF FIXED VARIABLES];
RUN;
PROC GLM DATA=[DATA NAME];
CLASS [LIST OF CLASS VARIABLES];
MODEL [DEPENDENT VARIABLE]=[VARIABLE OF INTEREST];
MEANS [VARIABLE OF INTEREST]/TUKEY;
RUN;
```

In this case the list of fixed variables included P_{max} and D_c and the variable of interest was t_h. This code tests whether the different levels of t_h are significantly different under given fixed levels of P_{max} and D_c. Table (5-3) in the text shows the result of the test.

LIST OF REFERENCES

ASAE Standards. 1995. American Society of Agricultural Engineers. St. Joseph, MI.

Bagnall, L.O. 1973. Processing, chemical composition and nutritive value of aquatic weeds. Florida Water Resource Center. Publication No. 25.

Balatinecz, J.J. 1983. The potential role of densification in biomass utilization. *In* Cote, W.A. (ed.). Biomass Utilization. Plenum Press, New York.

Balk, W.A. 1962. Energy requirements for dehydrating and pelleting coastal bermudagrass. ASAE paper No. 62-601.

Balk, W.A. 1965. Factors affecting pellet-mill performance with coastal bermudagrass. ASAE paper No. 65-109.

Ballard-Tremeer, G. and H.H. Jawurek. 1996. Comparison of five rural, wood-burning cooking devices: efficiencies and emissions. Biomass and Bioenergy 11(5):419-430.

Beck, S.R. and J.E. Halligan. 1980. Thermochemical conversion of agricultural residues. *In* Shuler, M.L. (ed.). Utilization and Recycle of Agricultural Wastes and Residues. CRC Press, Boca Raton, FL.

Bellinger, P.L. and H.F. McColly. 1961. Energy requirements for forming hay pellets. Agricultural Engineering 42:180-181, 244-247, 250.

Bhattacharia, S.C., S. Sett and R.M. Shrestha. 1989. State of the art for biomass densification. Energy Sources 11(3):161-182.

Bilanski, W.K., V.A. Graham and J.A. Hanusiak. 1985. Mechanics of bulk forage deformation with application to wafering. Transactions of the ASAE 28(3):697-702.

Braunstein, H.M., P. Kanciruk, R.D. Roop, F.E. Sharples, J.S. Tatum, and K.M. Oakes. 1981. Biomass Energy Systems and the Environment. Pergamon Press, New York.

Bruhn, H.D. 1955. Pelleting grain and hay mixtures. Agricultural Engineering 35(5):330- 331.

Bruhn, H.D., A. Zimmerman and R.P. Niedermeir. 1959. Developments in pelleting forage crops. Agricultural Engineering 40(4):204-207.

Bushmeyer, W.R., D.E. Krause and C.J. Rath.1969. Development of a roll wafering machine. ASAE paper No. 69-163.

Butler, J.L. 1965. Energy comparisons of processing coastal bermudagrass and alfalfa. Transactions of the ASAE 8(2):175-176, 179.

Butler, J.L. and H.F. McColly. 1959. Factors affecting the pelleting of hay. Agricultural Engineering 48(4):442-446.

Chancellor, W.J. 1961. Formation of hay wafers with impact loads. ASAE paper No. 61- 620.

Cheremisinoff, N.P., P.N. Cheremisinoff and F. Ellerbusch. 1980. Biomass: applications, technology, and production. *In* Powers, P.N. and W. Meier, JR. (eds.). Energy, Power, and Environment. Marcel Dekker, Inc., New York.

Claar, P.W., W.F. Buchele and S.J. Marley. 1980. Development of a concentric-vortex agricultural-residue furnace. Agricultural Energy Vol. 2. American Society of Agricultural Engineers, St. Joseph, MI.

Culp, A.W. and Jr. 1991. Principles of Energy Conversion. McGraw-Hill, Inc., New York.

Day, C.L. 1964. A device for measuring voids in porous materials. Agricultural Engineering 45(1):36-37.

Day, C.L. 1965. Effect of moisture content, depth of storage, and length of cut on bulk density of alfalfa hay. ASAE paper No. 65-811.

Dobie, J.B.1959. Engineering appraisal of hay pelleting. Agricultural Engineering 40(2):76-77, 92.

Dobie, J.B. 1960. Production of hay wafers. Agricultural Engineering 41(6):366-369.

Elliott, R.N. 1980. Wood combustion. *In* Levi, M.P. and O'Grady, M.J. (eds.). Decision Maker's Guide to Wood Fuel for Small Industrial Energy Users. Solar Energy Research Institute., Golden, CO.

Erikson, S. and M. Prior. 1990. The Briquetting of Agricultural Wastes for Fuel. FAO Environment and Energy Paper 11.

Faborode, M.O. and J.R. O'Callaghan. 1986. Theoretical analysis of the compression of fibrous agricultural residues. Journal of Agricultural Engineering Research 35:175-191.

Faborode, M.O. and J.R. O'Callaghan. 1987. Optimizing the compression/briquetting of fibrous agricultural materials. Journal of Agricultural Engineering Research 38:245-262.

Faborode, M.O. and J.R. O'Callaghan. 1989. A rheological model for the compaction of fibrous agricultural materials. Journal of Agricultural Engineering Research 42: 165-178.

Fluck, R. and C.D. Baird. 1980. Agricultural Energetics. Avi Publishing Co, Inc. Westport, CT.

Gardner, C.S. and G.M. Prine. 1986. Phytomass yield of elephantgrass as affected by fertilizer nitrogen and cool-season legume intercrop. Soil and Crop Science Soc. of Fla., Proc., Vol. 46:46-51.

Graham, V.A. and W.K. Bilanski. 1984. Non-linear viscoelastic behavior during forage wafering. Transactions of the ASAE 28(3):1661-1665.

Green, A., H. Van Ravenswaay, J. Wagner, B. Green, T. Cherry and D. Clauson. 1991.Co-feeding and co-firing biomass with non-hazardous waste and natural gas. Bioresource Technology 36:215-221.

Gustafson, A.S. and W.J. Kjelgaard. 1963. Hay pellet geometry and stability. Agricultural Engineering 44(8):422-425.

Gustafson, M.L. 1959. The durability test-a key to handling wafers and pellets. ASAE paper No. 59-621.

Haase, S. and J. Whittier. 1994. Wood pelletization sourcebook. Bioenergy '94. 6th. National Bioenergy Conference, Reno, NV.

Hall, G.E., and W.C. Hall. 1967. Heated-die wafer formation of alfalfa and bermudagrass. ASAE paper No. 67-682.

Headley, V.E. 1968. Equilibrium moisture content of some pelleted feed and its effect on pellet durability index. ASAE paper No. 68-345.

Heldman, D.R. 1975. Food Process Engineering. Avi Publishing CO, Inc., Westport, CT.

Hellwig, R.E., and J.L. Butler. 1971. Power requirements for pelleting peanut hulls. A paper presented at the Southeast Region ASAE meeting, Jacksonville, FL, January 31- February 3.

Henderson, S.M. and R.L. Perry. 1976. Agricultural Process Engineering. The Avi Publishing Co., Inc. Westport, CT.

Hill, B. and D.A. Pulkinen, 1988. A study of factors affecting pellet durability and pelleting efficiency. Saskatchewan Dehydrator Association.

Holman, J.P. 1986. Heat Transfer. McGraw-Hill Book Company, New York.

Howell, J.R. and R.O. Buckius. 1987. Fundamentals of Engineering Thermodynamics. McGraw-Hill Book Company, New York.

Huang, B.K. and R.R. Yoerger. 1961. Maceration as a pretreatment in hay wafering. Transactions of the ASAE 4(1):69-71.

Huff, E.R. 1980. Effect of size, moisture content, and environment temperatures on burning times of wood cubes. Agricultural Energy, Vol. 2. American Society of Agricultural Engineers, St. Joseph, MI.

Hundtoft, E.B. and F.H. Buelow. 1971. An axial stress-strain relationship for bulk alfalfa. Journal of Agricultural Engineering Research 16(1):32-45.

Jenkins, B.M., L.L. Baxter, T.R. Miles, T.R. Miles, Jr., L.L. Oden, R.W. Bryers and E. Winther. 1994. Composition of ash deposits in biomass fueled boilers: results of full scale experiments and laboratory simulations. ASAE paper No. 946007.

Johnston, D. 1995. Pellets: ashes, ashes. Alternative Energy Retailer 15(3):1-19.

Joshi, V., C. Venkataraman and D.R. Ahuja. 1989. Emissions from burning biofuels in metal cookstoves. Environmental Management 13(6):763-772.

Khankari, K.K., M. Shrivastava and R.V. Morey. 1989. Densification characteristics of rice hulls. ASAE paper No. 89-6093.

Kjelgaard, W.L., D.A. Ashcroft, J.R. Graham, W.O. Stewart, R.E. Stone and Y. Yang. 1976. Compression and other properties of chopped forages. Ag. Experimental Station, Bulletin 807, Penn State Univ., University Park, PA.

Marchant, W.T. 1961. A small hydraulic cubing machine for farms. Journal of Agricultural Engineering Research 6(4):59- 65.

Miles, T.R. 1992. Operating experience with ash deposition in biomass combustion systems. A paper presented at the Biomass Combustion Conference, Reno, NV.

Miles, T.R. 1995. Biomass feedstocks for gasification. A paper presented at the IEA meeting, Portland, OR.

Miles, T.R. and T.R. Miles, Jr. 1980. Densification systems for agricultural residues. *In* Jones, J.L. and S.B. Radding (eds.). Thermal Conversion of Solid Waste and Biomass. American Chemical Society, Washington, D.C.

Miles, R.T., R.T. Miles, Jr., L. Baxter, B.M. Jenkins and L. Oden. 1993. Alkali slagging problems with biomass fuels. A paper presented at the First Biomass Conference of the Americas, Burlington, VM.

Mohsenin, N.N. 1986. Physical Properties of Plant and Animal Materials: Structure, Physical Characteristics and Mechanical Properties. Gordon and Breach, New York.

Mohsenin, N. and J. Zaske. 1976. Stress relaxation and energy requirements in compaction of unconsolidated materials. Journal of Agricultural Engineering Research 21:193-205.

Molitorisz, J. 1968. Development and analysis of the rolling-compressing wafering process. ASAE paper No. 68-634.

Molitorisz, J. and H.F. McColly. 1970. Analyses of channel systems for rolling-compressing hay wafers. ASAE paper No. 70-621.

Moustafa, S.M., B.A. Stout and W.A. Bradley. 1966. Theoretical modeling of the wheat plant. ASAE paper No. 66-340.

O'Dougherty, M.J. and J.A. Wheeler.1984. Compression of straw to high densities in closed cylindrical dies. Journal of Agricultural Engineering Research 29:61-72.

O'Grady, M.J., R.C. Farley and R. Arnold. 1980. Pelletized wood. *In* Levi, M.P. and M.J., O'Grady (ed.). Decision Maker's Guide to Wood Fuel for Small Industrial Energy Users. Solar Energy research Institute., Golden, CO.

Ott, L. 1988. An Introduction to Statistical Methods and Data Analysis. PWS-Kent Publication, Co., Boston, MA.

Parikh, P.P., K.B. Reddy and P.K. Banerjee. 1994. On Proximate analysis procedures for biomass characterization. ASAE paper 946013.

Petrie, J.G. and S. Baldwin. 1992. Devolatilization and combustion of pelletized and briquetted wastes. Journal of the Institution of Energy 65(465):185-191.

Pfost, H.B. 1961. Particle-size reduction during pelleting. ASAE paper No. 61-625.

Pickard, G.E., W.M. Roll and J.H. Ramser. 1961. Fundamentals of hay wafering. Transactions of the ASAE 4(1):65-68.

Pryne, R.K. 1985. A hand operated process for making fuel briquettes from fibrous wastes. Vita News. January, pp. 11-13.

Rajvanshi, A.K. 1985. Potential briquettes from farm residues as rural energy source. Changing Villages 7:123-141.

Reece, F.N. 1965. Temperature, pressure, and time relationships in forming dense hay wafers. ASAE paper No. 65-638.

Reed, T.B. and B. Bryant. 1978. Densified Biomass: A New Form of Energy. Solar Energy Research Institute. Golden, CO.

Reed, T.B., Trezek, G. and L. Diaze. 1980. Biomass densification energy requirements. *In* Jones, J.L. and S.B. Radding (ed.). Thermal Conversion of Solid Waste and Biomass. American Chemical Society, Washington, D.C.

Rehkugler, G.E. and W.F. Buchele. 1967. Influence of stems in alfalfa forage on the formation of wafers. Journal of Agricultural Engineering Research 12(4): 285-292.

Rehkugler, G.E. and W.F. Buchele. 1969. Biomechanics of forage wafering. Transactions of the ASAE 12(1):1-8.

Ross, I.J. and C.F. Kiker. 1967. Some physical properties of dried citrus pulp. ASAE paper No. 66-807.

Rossi, A. 1984. Fuel characteristics of wood and nonwood biomass fuels. *In* Tillman, D.A. and E.C. Jahn (eds.). Progress in Biomass Conversion, Vol. 5. Academic Press, New York.

Rundell, G.C. and G.E. Fairbanks. 1967. Effect of hay length on wafer durability. ASAE paper No. 67-681.

Sah, P.C., B. Singh and U. Agrawal. 1980. Compaction behavior of straw. Journal of Agricultural Engineering-India 18(1):89-96.

Salter, D.E. 1982. Production of fuel pellets by the densification of biomass. Energex'82:1130-1132.

Shafizadeh, F. 1981. Basic principles of direct combustion. *In* Sofer, S.S. and O.R. Zaborski (ed.). Biomass Conversion Processes for Energy and Fuels. Plenum Press, New York.

Shafizadeh, F. 1982. Chemistry of pyrolysis and combustion of wood. *In* Sarkanen, K.V., D.A. Tillman and E.C. Jahn (ed.). Progress in Biomass Conversion. Vol. 3. Academic Press, New York.

Shepperson, G. and J.K. Grundey. 1962. Experiments in the production of hay wafers. Journal of agricultural Engineering Research 7(2):105-111.

Singh, R., R.C. Maheshwari and T.P. Ojha. 1980. Development of a husk fired furnace. Journal of Agricultural Engineering Research 25(2):109-120.

Sitkei, G. 1986. Mechanics of Agricultural Materials. Elsevier Science Publishing CO., Inc. New York.

Smith, I.E., S.D. Probert, R.E. Stokes and R.J. Hansford. 1977. The briquetting of wheat straw. Journal of Agricultural Engineering Research 22:105-111.

Smith, K.R. 1987. Biofuels, Air Pollution, and Health: A Global Review. Plenum Press, New York.

Smith, M.R. 1987. Harvesting and handling of biomass energy crops. Proceedings of the International Symposium on Agricultural Mechanization and International Cooperation, April, pp. 215-218. Tokyo, Japan.

Tillman, D.A., A.J. Rossi, and W.D. Kitto. 1981. Wood Combustion: Principles, Processes, and Economics. Academics Press, New York.

Tuhoy, P. and M. Juhasz. 1994. Direct combustion of materials. Bioenergy '94:84-91. The Sixth National Bioenergy Conference, Reno, NV.

Waelti, H, and J.B. Dobie. 1971. Cubability of rice straw as affected by various binders. ASAE paper 71-115.

White, L.P. and L.G. Plaskett. 1981. Biomass as Fuel. Academic Press, New York.

Wilkie, A., M. Goto, F.M. Bordeaux and P.H. Smith. 1986. Enhancement of anaerobic methanogenesis from napiergrass by addition of micronutrients. Biomass 11:135-146.

Willits, D.H., J.M. Myers and I.J. Ross. 1969. A Low pressure pelleting process for citrus pulp. Transactions of the ASAE 12(4):443-447, 451.

Winter, R.M., J.R. Clough and D.W. Pershing. 1983. Formation of NO and particulates during suspension-phase wood combustion. *In* Tillman, D.A. and E.C. Jahn (eds.). Progress in Biomass Conversion, Vol. 4. Academic Press, New York.

Witte, D. and D. Hunt. 1961. Energy requirements for extruding hay. ASAE paper No. 61-621.

Woodard, K.R. and G.M. Prine. 1992. Dry matter accumulation of elephantgrass, energycane, elephantmillet in a subtropical climate. Crop Science 33(4):818-824.

Woodard, K.R., G.M. Prine and W.R. Ocumpaugh. 1985. Techniques in the establishment of elephantgrass. Soil and Crop Science Society of Florida Proceedings, Vol. 44:216-221.

Woodard, K.R., G.M. Prine and S. Bachrein. 1993. Solar energy recovery by elephantgrass, energycane and elephantmill canopies. Crop Science 33(4):824-830.

BIOGRAPHICAL SKETCH

Mohamad Mofleh was born in Irbid, Jordan, in 1961. He received a B.S. in mechanical engineering in 1985 from Yarmouk University, Irbid, Jordan. After his B.S., he worked as a teaching assistant in Amman Polytechnic, Jordan, until 1988. He then enrolled in the Jordan military for two years. Mr. Mofleh attended graduate school at Kansas State University in the Department of Agricultural Engineering in the Fall, 1991 where he got a Master of Engineering degree in the Summer, 1993. From the Fall, 1993, he was enrolled in the graduate program in the Department of Agricultural and Biological Engineering at the University of Florida.

I certify that I have read this study and that in my opinion it conforms to acceptable standards of scholarly presentation and is fully adequate, in scope and quality, as a dissertation for the degree of Doctor of Philosophy.

Larry O. Bagnall, Chair
Professor of Agricultural and Biological Engineering

I certify that I have read this study and that in my opinion it conforms to acceptable standards of scholarly presentation and is fully adequate, in scope and quality, as a dissertation for the degree of Doctor of Philosophy.

Lawrance N. Shaw
Professor of Agricultural and Biological Engineering

I certify that I have read this study and that in my opinion it conforms to acceptable standards of scholarly presentation and is fully adequate, in scope and quality, as a dissertation for the degree of Doctor of Philosophy.

Richard C. Fluck
Professor of Agricultural and Biological Engineering

I certify that I have read this study and that in my opinion it conforms to acceptable standards of scholarly presentation and is fully adequate, in scope and quality, as a dissertation for the degree of Doctor of Philosophy.

Clyde F. Kiker
Professor of Food and Resource Economics

I certify that I have read this study and that in my opinion it conforms to acceptable standards of scholarly presentation and is fully adequate, in scope and quality, as a dissertation for the degree of Doctor of Philosophy.

Alex E. Green
Graduate Research Professor of Mechanical Engineering

This dissertation was submitted to the Graduate Faculty of the College of Engineering and to the Graduate School and was accepted as partial fulfillment of the requirements for the degree of Doctor of Philosophy.

August, 1997

Winfred M. Phillips
Dean, College of Engineering

Karen A. Holbrook
Dean, Graduate School